

CALCULATION OF SURFACE CURRENT
ON PERFECTLY CONDUCTING BODIES
OF ARBITRARY SHAPE

Kharavuth Khemayodhin

Library
Naval Postgraduate School
Monterey, California 93946

NAVAL POSTGRADUATE SCHOOL

Monterey, California



THESIS

CALCULATION OF SURFACE CURRENT
ON PERFECTLY CONDUCTING BODIES
OF ARBITRARY SHAPE

by

Kharavuth Khemayodhin

December, 1974

Thesis Advisor:

R.W. Adler

Approved for public release; distribution unlimited.

Prepared for:

Air Force Weapons Laboratory
Kirtland AFB, New Mexico 87117

U164893

NAVAL POSTGRADUATE SCHOOL
Monterey, California

Rear Admiral Isham W. Linder

Jack R. Borsting
Provost

This thesis was prepared in conjunction with research support in part by Air Force Weapons Laboratory under Project Order Number 75-002, 13 May 74.

Reproduction of all or part of this report is authorized.

Released as a
Technical Report by:

REPORT DOCUMENTATION PAGE		READ INSTRUCTIONS BEFORE COMPLETING FORM	
1. REPORT NUMBER NPS-52AB74123		3. RECIPIENT'S CATALOG NUMBER	
2. GOVT ACCESSION NO.		5. TYPE OF REPORT & PERIOD COVERED Engineer's December 1974	
4. TITLE (and Subtitle) Calculation of Surface Current on Per- fectly Conducting Bodies of Arbitrary Shape		6. PERFORMING ORG. REPORT NUMBER	
7. AUTHOR(•) Kharavuth Khemayodhin in conjunction with Richard William Adler		8. CONTRACT OR GRANT NUMBER(•) 75-002	
9. PERFORMING ORGANIZATION NAME AND ADDRESS Naval Postgraduate School Monterey, California 93940		10. PROGRAM ELEMENT, PROJECT, TASK AREA & WORK UNIT NUMBERS	
11. CONTROLLING OFFICE NAME AND ADDRESS Air Force Weapons Laboratory Kirtland AFB, New Mexico 87117		12. REPORT DATE December 1974	
14. MONITORING AGENCY NAME & ADDRESS (if different from Controlling Office)		13. NUMBER OF PAGES 82	
		15. SECURITY CLASS. (of this report) Unclassified	
		15a. DECLASSIFICATION/DOWNGRADING SCHEDULE	
16. DISTRIBUTION STATEMENT (of this Report) ** Approved for public release; distribution unlimited.			
17. DISTRIBUTION STATEMENT (of the abstract entered in Block 20, if different from Report)			
18. SUPPLEMENTARY NOTES			
19. KEY WORDS (Continue on reverse side if necessary and identify by block number) Surface Current; Conducting Bodies			
20. ABSTRACT (Continue on reverse side if necessary and identify by block number) A numerical method was developed to solve for current distri- bution on perfectly conducting bodies due to arbitrarily impressed fields. The formulation of the problem was based on the method of moments in conjunction with the reaction matching technique. The current distribution was assumed to be linear combination of two dimensional piecewise sinusoidal functions. A computer pro- gram was written to demonstrate the feasibility of this technique			

for plane wave scattering problems.

Calculation of Surface Current
on Perfectly Conducting Bodies
of Arbitrary Shape

by

Kharavuth Khemayodhin
First Lieutenant, Royal Thai Army
B.S., Virginia Military Institute, 1969

Submitted in partial fulfillment of the
requirements for the degree of

ELECTRICAL ENGINEER

from the

NAVAL POSTGRADUATE SCHOOL
December 1974

71.25.3
3062
C. 1

ABSTRACT

A numerical method was developed to solve for current distribution on perfectly conducting bodies due to arbitrarily impressed fields. The formulation of the problem was based on the method of moments in conjunction with the reaction matching technique. The current distribution was assumed to be linear combination of two dimensional piecewise sinusoidal functions. A computer program was written to demonstrate the feasibility of this technique for plane wave scattering problems.

TABLE OF CONTENTS

I.	INTRODUCTION -----	10
II.	THEORETICAL FORMULATION -----	12
	A. STATEMENT OF THE PROBLEM -----	12
	B. THE ELECTROMAGNETIC BOUNDARY VALUE PROBLEM ---	12
	C. THE METHOD OF MOMENTS -----	14
	D. APPLICATION OF THE REACTION MATCHING TECHNIQUE	15
	E. SELECTION OF SOLUTION TECHNIQUE -----	18
	1. Discussion of Various Techniques -----	18
	2. Two Dimensional Piecewise Sinusoidal Reaction Matching Technique -----	19
III.	NUMERICAL TECHNIQUES -----	26
	A. NUMERICAL INTEGRATION -----	26
	B. CALCULATION OF THE COUPLING TERMS -----	28
	C. CALCULATION OF THE DRIVE TERMS -----	31
IV.	CALCULATION OF MUTUAL IMPEDANCE BETWEEN TWO FILA- MENTARY DIPOLES WITH PIECEWISE SINUSOIDAL CURRENT DISTRIBUTION -----	36
V.	NUMERICAL RESULTS -----	45
	A. RECTANGULAR PLATE -----	45
	B. SQUARE PLATE -----	51
	C. HOLLOW CYLINDRICAL TUBE -----	63
	D. L-SHAPED HOLLOW CYLINDRICAL TUBE -----	69
VI.	CONCLUSIONS -----	74
	LIST OF REFERENCES -----	77
	INITIAL DISTRIBUTION LIST -----	79

LIST OF TABLES

1.	MUTUAL IMPEDANCE OF CENTER-FED PLANAR SURFACE DIPOLES---	33
2.	MUTUAL IMPEDANCE BETWEEN DIPOLES IN FIGURE 10 BY----- THREE METHODS	44
3.	CURRENT ON RECTANGULAR PLATE OF FIGURE 11-----	47
4.	CURRENT ON SQUARE PLATE OF FIGURE 13 FOR BROADSIDE ----- INCIDENCE	53

LIST OF DRAWINGS

Figure No.		Page
1.	DIVISION OF THE SURFACE INTO INTERCONNECTING ----- RECTANGULAR PATCHES	21
2.	TWO DIMESIONAL PIECEWISE SINUSOIDAL INTERPOLATION	22
3.	COORDINATE SYSTEM FOR DISTORED RECTANGULAR PATCH -	23
4.	THREE TYPES OF BASIS EXPANSION FUNCTIONS -----	24
5.	TWO SURFACE MONOPOLES -----	29
6.	COUPLED SURFACE DIPOLES -----	32
7.	SPECIFICATION OF A PLANE WAVE -----	35
8.	ARRANGEMENT OF TWO ARBITRARILY ORIENTED MONOPOLES	37
9.	ELECTRIC FIELD ON MONOPOLE "a" -----	39
10.	DIPOLE CONFIGURATION FOR TABLE 2 -----	43
11.	DESCRIPTION OF RECTANGULAR PLATE PROBLEM -----	46
12.	THE ISOMETRIC PLOT OF CURRENT ON THE RECTANGULAR PLATE OF FIGURE 11 -----	49
13.	DESCRIPTION OF SQUARE PLATE PROBLEM -----	52
14.	THE ISOMETRIC PLOT OF CURRENT OF THE SQUARE PLATE OF FIGURE 13 -----	56
15.	CURRENTS ON SQUARE PLATE FOR BROADSIDE INCIDENCE COMPARED WITH THOSE CALCULATED BY RAMAT-SAMII AND MITTRA [10] -----	62
16.	DESCRIPTION OF HOLLOW CYLINDRICAL TUBE PROBLEM ---	64
17.	THE ISOMETRIC PLOT OF CURRENT ON HOLLOW CYLINDRICAL TUBE OF FIGURE 16 -----	66

18.	CURRENTS ON HOLLOW CYLINDRICAL TUBE COMPARED WITH THOSE CALCULATED BY KAO [18] FOR THE SAME GEOMETRY BUT WITH CIRCULAR CROSS SECTION -----	68
19.	DESCRIPTION OF L-SHAPED HOLLOW CYLINDRICAL TUBE -----	70
20.	THE ISOMETRIC PLOT OF CURRENT ON L-SHAPED HOLLOW CYLINDRICAL TUBE OF FIGURE 9 -----	72

ACKNOWLEDGEMENT

The author wishes to express sincere appreciation to Dr. J.H. Richmond and Dr. R.W. Adler for their assistance and guidance throughout this thesis.

I. INTRODUCTION

The most important step in antenna and scattering problems is the obtaining, assuming, or approximating of the current distribution. Once all the electric and magnetic currents are known, all other electromagnetic quantities can be readily calculated from them. To obtain the current distribution exactly, one has to solve the electromagnetic boundary value problem. This is possible only for simple geometries. For most problems, only approximate solutions are possible. The method of moments presented by Harrington [1,2] makes it possible to obtain an approximate solution of the boundary value problem using high speed and large storage computers.

The thin wire problem was among the first to be extensively investigated. This was logical since current on a thin wire is a one dimensional quantity. Many methods for the thin wire problem were developed. They are all based on the method of moments, but various techniques were used to achieve simplicity and efficiency. One of the most efficient methods is the piecewise sinusoidal reaction matching technique (PSRMT) developed by Richmond [3,4].

The next logical step was to solve problems with two dimensional current distribution found on surfaces and perfectly conducting bodies. One of the first methods tried was modeling surfaces by a wire grid mesh [5]. The wire grid model seems to be adequate for calculation of the

echo area and radiation patterns, but it is questionable that the current on a surface can be approximated by wire grid currents. The surface current model is more realistic. The bases for surface current may be divided into two categories: the entire domain type and the subdomain type (current patch model). The entire domain type is characterized by complexity in formulation, but if bases are properly chosen a small number of basis functions are required. The current patch model is more adaptable to arbitrarily shaped bodies, but the number of patches increases linearly as the surface area.

In this thesis, the PSRMT was extended for two dimensional current. First, the surface of conducting bodies are divided into rectangular or almost rectangular patches. Values of current at vertices of patches are unknowns to be found. Currents elsewhere are to be determined by interpolation with a piecewise sinusoidal function in two dimensions. The system of linear equations are formed by Galerkin's method. Finally, the linear equations are solved to obtain the values of current at the vertices of patches.

The technique developed in this thesis is a modification of a technique used by Richmond and Wang in their work on scattering bodies [6].

II. THEORETICAL FORMULATION

A. STATEMENT OF THE PROBLEM

A perfectly conducting body, having outer surface S , surrounded by a linear, homogeneous, isotropic, and infinitely extended medium characterized by permeability μ and permittivity ϵ , is excited by the impressed electric and magnetic fields (\bar{E}^i, \bar{H}^i) . Electric Current \bar{J}^S is induced on S to satisfy the boundary condition. The objective of this thesis is to find \bar{J}^S .

B. THE ELECTROMAGNETIC BOUNDARY VALUE PROBLEM

Inside a perfectly conducting body the electric field, magnetic field, electric current and magnetic current vanish. On the surface the tangential component of the electric field, the normal component of the magnetic field, and the magnetic current vanish, and only electric current can exist. The proof of these properties can be found in standard electromagnetic text books [7]. The total field everywhere can be found from

$$\bar{E} = \bar{E}^i + \bar{E}^S \quad (1)$$

$$\bar{E}^S = -j\omega\bar{A} - \nabla V \quad (2)$$

$$\bar{A} = \mu \int_S \bar{J}^S \frac{e^{-jkR}}{4\pi R} ds \quad (3)$$

$$V = \frac{-1}{j\omega\mu} \nabla \cdot \bar{A} \quad (4)$$

$$\bar{H} = \frac{-1}{j\omega\mu} \nabla \times \bar{E} \quad (5)$$

where $k = \omega \sqrt{\mu\epsilon}$.

(\bar{E}, \bar{H}) are the total electric and magnetic fields everywhere, \bar{E}^i is the impressed electric field, \bar{E}^s is the scattered electrical field due to the scattered current \bar{J}^s , \bar{A} is the magnetic vector potential, V is the electric scalar potential, R is the distance from the source point to the field point, ds is the differential surface area, S is the surface of the conducting body, and k is the wave number. The time dependent factor $e^{j\omega t}$ of the field and source terms is suppressed. The boundary condition for the problem is

$$\bar{n} \times \bar{E} \Big|_{\text{on } S} = 0 \quad (6a)$$

$$\text{or } \bar{E} \Big|_{\text{inside } S} = 0 \quad (6b)$$

where \bar{n} is the unit vector pointing outward and normal to the surface S . Equations (1) through (6) constitute the integro-differential equation and boundary conditions for the problem. The unknown function to be found is \bar{J}^s . It can be shown by the uniqueness theorem that the solution of \bar{J}^s obtained from these equations is unique. The exact solution is possible when the surface S and the impressed field \bar{E}^i can be described in simple forms in some coordinate system. When the geometry of the conducting body is more complicated, only a numerical solution is practical.

C. THE METHOD OF MOMENTS

The method of moments as formulated by Harrington is now widely used for solving electromagnetic boundary value problems. The equation to be solved is in the form of an operator equation:

$$L(f) = g , \quad (7)$$

where f is the unknown function to be found, g is a known function, and $L(\cdot)$ is a linear operator. The first step is to make the approximation:

$$f \doteq \sum_{n=1}^N C_n f_n , \quad (8)$$

where c_n are constants and f_n are known functions, called basis expansion functions or bases. They must be linearly independent and satisfy boundary conditions not already included in (7). By the linearity of $L(\cdot)$, (7) becomes

$$\sum_{n=1}^N C_n L(f_n) = g . \quad (9)$$

Now define both a set of testing functions w_m , which are linearly independent among themselves, and a scalar product $\langle w_m, f_n \rangle$. Taking the scalar product of each side of (9) with w_m , linear equations of N unknowns are obtained. The c_n can be found by solving the system of linear equations:

$$\sum_{n=1}^N a_{mn} c_n = b_m \quad m=1,2,\dots, M \quad (10)$$

$$a_{mn} = \langle w_m, L(f_n) \rangle$$

$$b_m = \langle w_m, g \rangle$$

$$M \geq N.$$

One should consider the following facts when applying the method of moments:

(1) The bases should be defined such that the approximation in (8) converges rapidly to the true solution as N increases.

(2) The testing functions and the scalar product should be defined such that the term a_{mn} can be calculated accurately and efficiently.

(3) The resulting linear equations should be well conditioned. That is, a small error in a_{mn} should not result in a large error in the solution of c_n . In a well conditioned matrix, the magnitude of the diagonal terms are large, and the magnitude of the other terms decrease rapidly as the "distance" from the diagonal increases.

(4) There is an upper limit to the value of N due to the finite storage, precision, and computing time of the computer.

D. APPLICATION OF THE REACTION MATCHING TECHNIQUE

The reaction concept was introduced by Rumsey [8] in 1954. Consider two sources which radiate in a linear, isotropic, and infinitely extended medium. Source "a" consists of currents (\bar{J}^a, \bar{M}^a) confined within volume V^a , and source "b" consists

of currents (\bar{J}^b, \bar{M}^b) confined within volume V^b . Source "a" alone in the medium radiates the fields (\bar{E}^a, \bar{H}^a) , and source "b" alone in the medium radiates the fields (\bar{E}^b, \bar{H}^b) . The reaction between sources "a" and "b" is defined as

$$\langle a, b \rangle = \iiint_{V^a} (\bar{J}^a \cdot \bar{E}^b - \bar{M}^a \cdot \bar{H}^b) dv \quad . \quad (11)$$

By the reciprocity theorem,

$$\langle a, b \rangle = \langle b, a \rangle \quad (12)$$

The reaction concept will be used later in this section. At this point the method of moment will be applied to the perfectly conducting body problem formulated in IIB. The boundary condition (and also the operator equation) is

$$-\bar{E}^S = \bar{E}^i \quad \text{inside } S \quad . \quad (13)$$

Since the fields inside S are zero, the conducting body can be removed and replaced by the medium (μ, ϵ) without affecting the field anywhere. The entire space is now filled with the medium (μ, ϵ) . The unknown function to be found is \bar{J}^S , and it is approximated to be

$$\bar{J}^S \doteq \sum_{n=1}^N c_n \bar{J}_n^S \quad , \quad (14)$$

where c_n are constants and \bar{J}_n^S are known current distribution functions. Let \bar{E}_n^S be the electric field radiated by \bar{J}_n^S in the medium (μ, ϵ) , and equation (15) becomes

$$-\sum_{n=1}^N c_n \bar{E}_n^s = \bar{E}^i, \text{ inside } S. \quad (15)$$

Now define a set of testing sources \bar{J}_m^t , confined within surface S_m , which are totally contained inside S . Take the dot product of \bar{J}_m^t with both sides of (15) and integrate over the surface S_m .

$$-\sum_{n=1}^N c_n \int_{S_m} \bar{J}_m^t \cdot \bar{E}_n^s ds = \int_{S_m} \bar{J}_m^t \cdot \bar{E}^i ds \quad (16)$$

It is necessary that the test sources \bar{J}_m^t are totally contained inside S since equation (15) is valid only in that region. The integration term on the left is recognized as the reaction between the m^{th} test source and the n^{th} expansion source. The right hand side is the reaction between m^{th} test source and the impressed field. The system of linear equation generated in this step is

$$-\sum_{n=1}^N c_n a_{mn} = b_m \quad m=1,2,\dots,N \quad (17)$$

$$a_{mn} = \int_{S_m} \bar{J}_m^t \cdot \bar{E}_n^s ds$$

$$b_m = \int_{S_m} \bar{J}_m^t \cdot \bar{E}^i ds$$

This is a special case of the reaction matching technique described by Richmond and Wang [6]. There is no fundamental difference between the reaction matching technique and the method of moments. The former has some useful physical interpretations attached to it where the latter is a general

mathematical method.

E. SELECTION OF A SOLUTION TECHNIQUE

1. Discussion of Various Techniques

There are many ways to select the basis expansion functions and the testing functions. Basis functions can be divided into two classes, the entire domain type in which in which each function exists over the whole surface, and the subdomain type or current patch model which each function exists only over a portion of the surface. For the entire domain type, a small number of basis functions can be used to obtain a good approximation of the current, but the computation involved is difficult. This type of basis is not readily adaptable to arbitrarily shaped objects, but has the potential of being the most efficient. The subdomain type is more suitable for arbitrary shapes. In most cases, bases are all the same function but displaced in space. For the testing functions there are two special cases. The testing function is the same as the expansion function in Galerkin's technique, while in point matching technique, the testing function is the impulse function. Galerkin's technique usually gives a better conditioned matrix and faster rate of convergence, but the calculation of the matrix elements may be more difficult. In all techniques, when the number of basis functions increases beyond a certain limit, the solution will diverge due to the finite precision of the computer.

Typical basis expansion functions are piecewise constant, piecewise linear, piecewise sinusoidal, and half-wave cosine. Tsai, Dudley, and Wilton [9] used piecewise constant bases and the point matching technique for the magnetic field integral equation formulated for a conducting rectangular box. Ramat-Samii and Mittra [10] used the same for an integral equation of a thin rectangular plate. Richmond and Wang [6] used half-wave cosine in the direction of current flow and piecewise constant in the orthogonal direction for bases and Galerkin's method in conjunction with the reaction matching technique in their work on conducting bodies of arbitrary shapes [6].

2. Two-Dimensional Piecewise Sinusoidal Reaction Matching Technique.

The piecewise sinusoidal reaction matching technique (PSRMT) was developed by Richmond [3] for thin-wire antennas and scatterers. It can be classified as a Galerkin's technique in which the bases are of subdomain type and assumed to be sinusoidal functions. It is one of the most efficient techniques for the thin wire problem. In this thesis, the PSRMT is extended to two-dimensional currents.

For simplicity the two-dimensional PSRMT will be formulated for a thin rectangular plate first. Consider a perfectly conducting thin rectangular plate of negligible thickness excited by an impressed field, \bar{E}^i . The surface is divided into interconnecting rectangular patches as shown in

figure 2, the values of current at vertices are assumed to be unknown constants c_{11} , c_{12} , c_{21} , c_{22} , and the current everywhere in the patch is assumed to be

$$J(y,z) = c_{11}g_1(y)h_1(z) + c_{12}g_1(y)h_2(z) + c_{21}g_2(y)h_1(z) + c_{22}g_2(y)h_2(z) \quad (18)$$

$$\text{where } g_1(y) = \frac{\sin k (y_2 - y)}{\sin k (y_2 - y_1)}$$

$$g_2(y) = \frac{\sin k (y - y_1)}{\sin k (y_2 - y_1)}$$

$$h_1(z) = \frac{\sin k (z_2 - z)}{\sin k (z_2 - z_1)}$$

$$h_2(z) = \frac{\sin k (z - z_1)}{\sin k (z_2 - z_1)}$$

When the surface cannot be divided into rectangular patches, slightly distorted flat rectangular patches are used. The interpolation functions are the same, but the coordinate system is distorted as shown in figure 3.

The current is required to be continuous over the whole surface. For thin plates the current that flows toward the edges must go to zero at the edges, but the current that flows parallel to the edges does not have to vanish. The basis expansion functions \bar{J}_n^S may be one of the three forms shown in figure 4. The domain of each basis function overlaps with that of its neighbors. Finally, the current on each patch is



FIGURE 1. DIVISION OF A SURFACE INTO INTERCONNECTING RECT-
ANGULAR PATCHES.

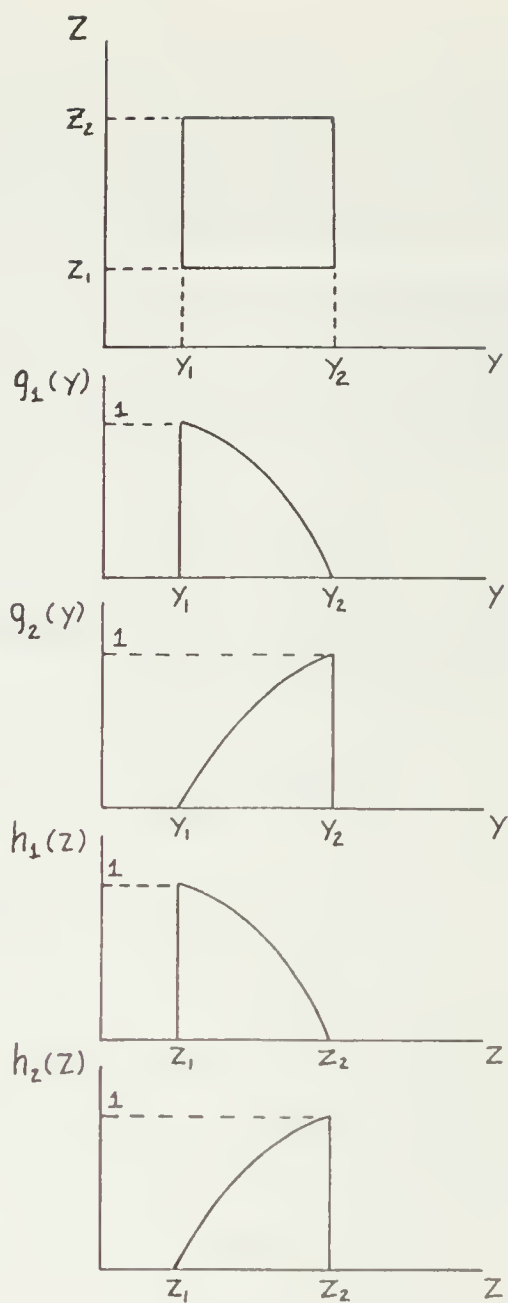


FIGURE 2. TWO-DIMENSIONAL PIECEWISE SINUSOIDAL INTERPOLATION.

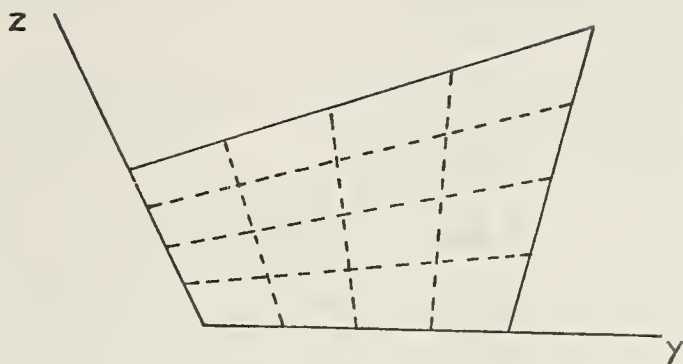


FIGURE 3. COORDINATE SYSTEM FOR DISTORTED RECTANGULAR PATCH.

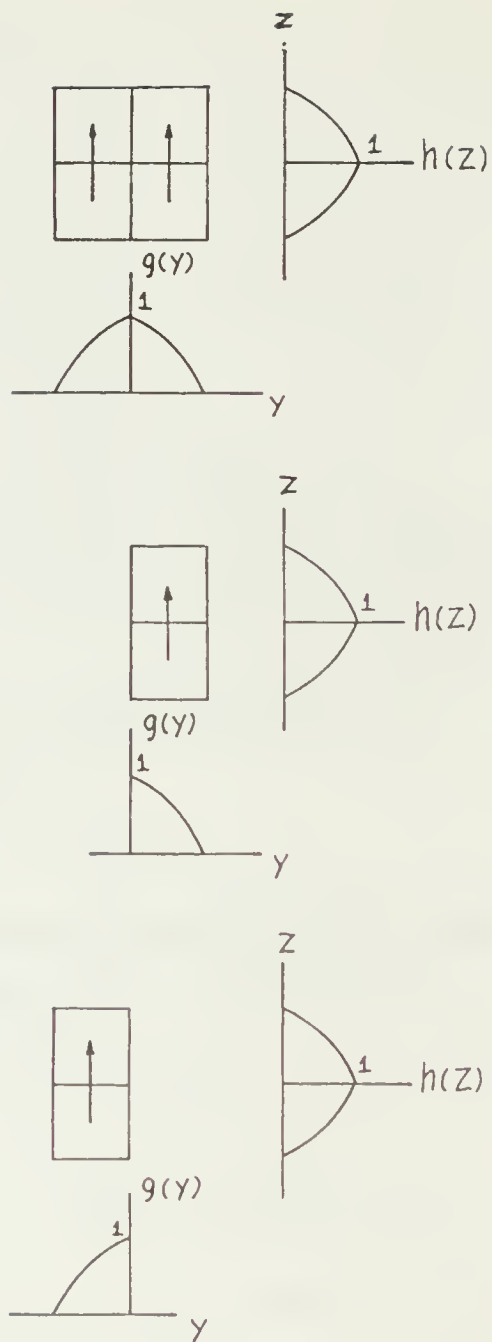


FIGURE 4. THREE TYPES OF BASIS EXPANSION FUNCTIONS.

$$\int_{x_0}^{x_0+6h} f(x) dx \doteq \frac{3h}{10} [f(x_0) + 5f(x_0+h) + f(x_0+2h) + 6f(x_0+3h) + f(x_0+4h) + 5f(x_0+5h) + f(x_0+6h)] . \quad (21)$$

While for the N-point Gaussian-Legendre method the formula is

$$\int_a^b f(x) dx \doteq (b-a) \sum_{n=1}^N w_i f(x_i) \quad (22)$$

$$\text{where } x_i = (b-a)u_i + \frac{b+a}{2}$$

The values of w_i and u_i can be found from references [11,12]. The Gaussian quadrature formula is the most efficient numerical integration formula in the sense that when an N-point formula is used, the result is exact if the integrand is a polynomial of degree $2N-1$ or less. Another feature is that the end points are not used as the sampling points; this feature is used to the advantage in the calculation of the coupling terms. For these reasons, the Gauss-Legendre formula was used in the computer program

Any numerical integration formula should not be used blindly. The nature of the integrand should be carefully investigated. When the N-point Gaussian formula is used, the result is good only when the integrand inside the interval can be well approximated by a polynomial of degree

2N-1 or less. For double integration, the numerical integration formula is applied twice

$$\int_c^d \int_a^b f(x,y) dx dy \doteq (d-c)(b-a) \sum_{i=1}^N \alpha_i \sum_{j=1}^M \beta_j f(x_i, y_j), \quad (23)$$

where α_i and β_j are weighting factors.

B. CALCULATION OF THE COUPLING TERMS

The coupling terms a_{mn} are the reactions between the m^{th} test source and the n^{th} expansion source. For the technique developed in this thesis the test source and the expansion source may be surface dipoles or quadrapoles. Both can be broken down as linear combinations of monopoles. Once the reaction between monopoles is formulated, the result can be extended to dipoles and quadrapoles. Consider two rectangular surface monopoles shown in figure 5. The assumed current distribution (equation(18)) can be put in the form:

$$\bar{J}^A(y,z) = g_A(y) h_A(z) \bar{a}_z \quad (24a)$$

$$\bar{J}^B(y',z') = g_B(y') h_B(z') \bar{a}_z, \quad (24b)$$

The reaction between monopoles A and B is

$$\langle a, b \rangle = \int_0^{L_A} \int_0^{W_A} \bar{J}^A(y,z) \cdot \bar{E}^B(y,z) dy dz, \quad (25)$$

where $\bar{E}^B(y,z)$ is the electric field generated by monopole B alone in the medium. Consider that monopole B consists of an infinite number of filamentary monopoles parallel

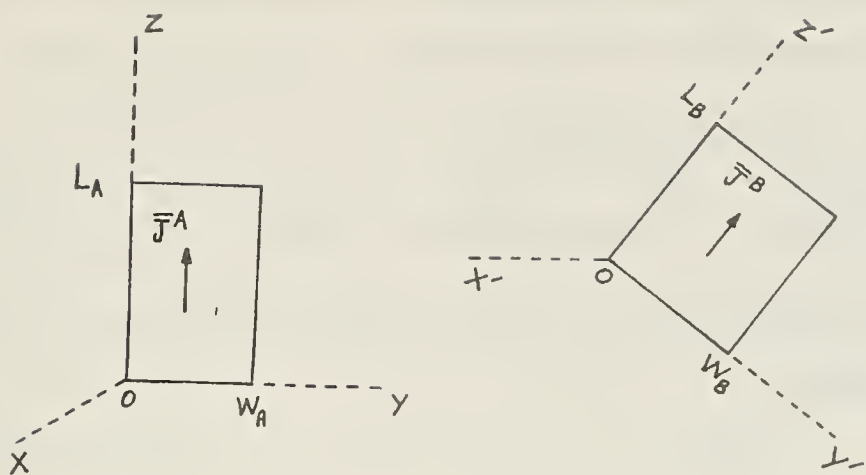


FIGURE 5. TWO SURFACE MONOPOLES.

to the z' axis. Let $\bar{E}_1^B(y, z, u)$ be the electric field at $x = 0$, generated by such filamentary monopole at $y' = u$, with current distribution $h_B(z')\bar{a}_z$, .

The $\bar{E}^B(y, z)$ can be expressed as

$$\bar{E}^B(y, z) = \int_0^W g_B(y') \bar{E}_1^B(y, z, y') dy' \quad . \quad (26)$$

Substituting in (25) and interchanging the order of integration gives

$$\begin{aligned} \langle a, b \rangle &= \int_0^W g_B(y') \left[\int_0^W g_A(y) \left[\int_0^{L_A} h_A(z) \bar{a}_z \cdot \bar{E}^B(y, z, y') dz \right] dy \right] dy' \quad . \quad (27) \end{aligned}$$

The term in the bracket is regionized as the reaction between two filamentary monopoles. One is on monopole A, parallel to the z axis, at the distance y from the origin of the (x, y, z) coordinate system with current distribution $h_A(z)\bar{a}_z$; and the other is on monopole B, parallel to the z' axis, at the distance y' from the origin of the (x', y', z') coordinate system, with current distribution $h_B(z')\bar{a}_z$, . Let $F(y, y')$ represent the term in the bracket; then (27) becomes

$$\langle a, b \rangle = \int_0^W g_B(y') \left[\int_0^W g_A(y) F(y, y') dy \right] dy' \quad . \quad (28)$$

Applying the numerical integration formula (23),

$$\langle a, b \rangle = W_A W_B \sum_{i=1}^N \sum_{j=1}^M \alpha_i \beta_j g_A(y_i) g_B(y_j) F(y_i, y_j) \quad (29)$$

In other words, the reaction between two surface monopoles in this case can be obtained from the reaction between filamentary monopoles. This technique was used by Richmond and Wang [6]. The current distribution of the filamentary monopoles is piecewise sinusoidal. The reaction between two filamentary monopoles with sinusoidal current distribution will be discussed later. Table 1 shows values of mutual impedance between dipoles in figure 6. The mutual impedance is defined as

$$Z_{ab} = \frac{-1}{I_{ao} I_{bo}} \langle a, b \rangle \quad (30)$$

where I_{ao} and I_{bo} are the total current flowing across the lines between monopoles.

For non-rectangular patches, the same method was used to find the coupling terms using the distorted coordinate system of figure 3. Equation (29) is not valid for non-rectangular monopoles, but when the monopoles are almost rectangular, the error is small.

C. CALCULATION OF THE DRIVE TERMS

The drive terms, b_m , are calculated from equation (17) using a numerical integration method. Since both \bar{J}_m^t and \bar{E}^i are known explicitly, the procedure is straight forward.

In the computer program, the impressed field is a plane wave traveling toward the origin from the direction (ϕ, θ) in spherical coordinates. The magnetic field at the origin

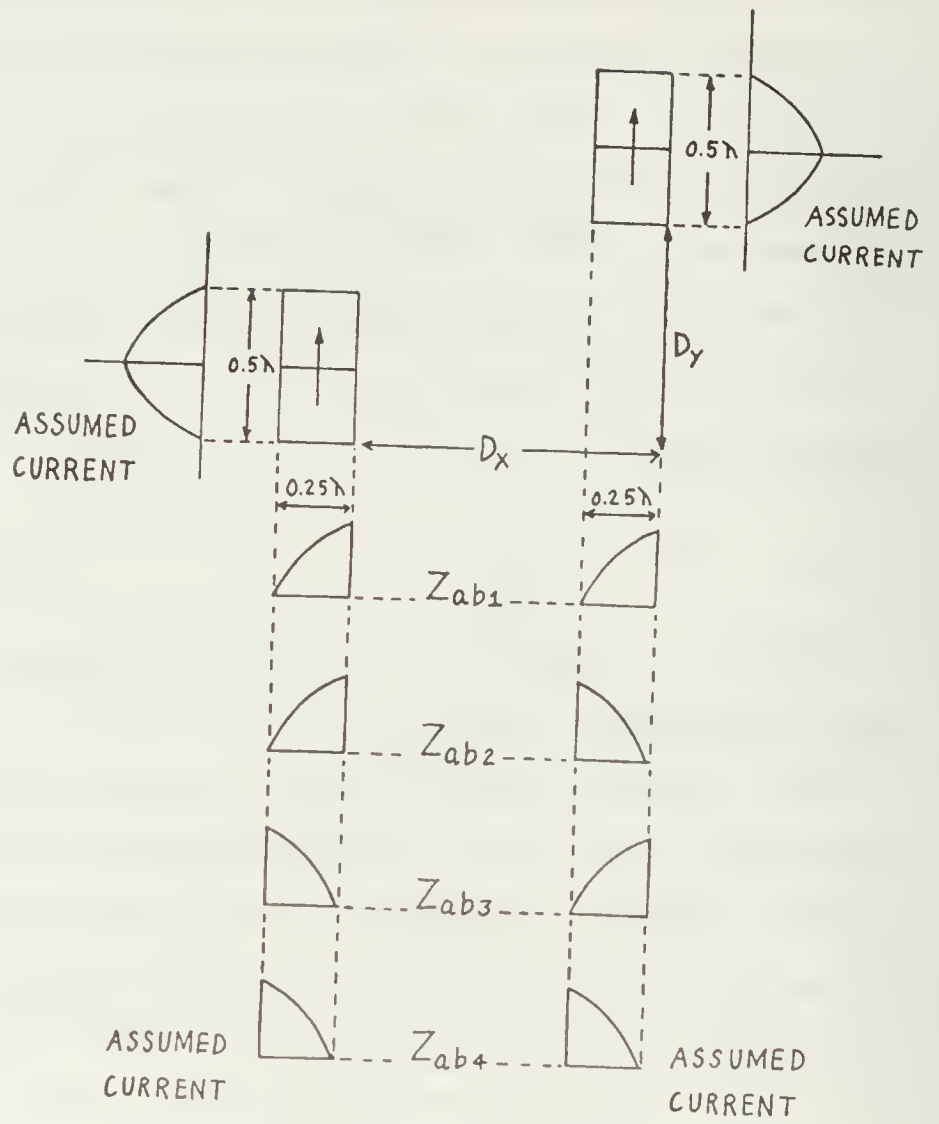


FIGURE 6. COUPLED SURFACE DIPOLES.

TABLE 1. MUTUAL IMPEDANCE OF CENTER-FED PLANAR SURFACE
DIPOLLES.

Dipoles and parameters are defined in figure 6.

0.75	1.37-j7.92	-2.92-j6.13	-6.26+j1.79	0.87+j7.35
	0.96-j7.85	-1.12-j7.12	-6.30-j0.82	-1.86+j6.92
	0.96-j7.85	-4.64-j4.53	-5.25+j4.25	3.62+j6.67
	1.37-j7.92	-2.92-j6.13	-6.26+j1.79	0.87+j7.34
0.5	24.39+j8.45	10.21-j10.19	-10.20-j6.99	-7.53+j9.47
	23.13+j5.20	16.39-j4.90	-6.16+j10.82	-10.80+j5.81
	23.13+j5.20	3.51-j12.55	-12.16-j2.08	-3.16+j11.46
	24.39+j8.45	10.21-j10.19	-10.20-j6.99	-7.53+j9.47
0.25	54.76+j69.66	29.89-j12.04	-10.42-j20.12	-16.44+j7.03
	52.60+j51.79	40.85+j7.48	-1.31-j24.44	-19.07-j0.17
	52.60+j51.79	17.64-j21.64	-16.46-j13.19	-11.48+j12.27
	54.76+j69.66	29.89-j12.02	-10.42-j20.12	-16.44+j7.03
0.0 z_{ab1}	69.05+j18.45	39.50-j24.05	-9.74-j27.61	-20.22+j4.92
z_{ab2}	66.50+j11.54	52.56-j11.11	1.70-j32.81	-22.37-j3.93
z_{ab3}	66.50+j11.54	24.81-j31.57	-17.71-j19.46	-15.21+j11.69
z_{ab4}	69.05+j18.45	39.50-j24.05	-9.74-j27.61	-20.22+j4.92
D_y / D_x	0.0	0.25	0.5	0.75

is one ampere/meter and has zero phase. The polarization is specified by angle P defined in figure 7. The (x'', y'', z'') coordinate system results from rotating the original coordinate system about the z axis by the angle ϕ then rotating about the new y axis by the angle $\frac{\pi}{2} - \theta$ so that the plane wave travels in the negative x'' direction. In this case the impressed electric field is

$$\bar{E}^i = e^{jkx''} \bar{a}_E \quad (30)$$

$$\text{where } x'' = (x \cos \phi + y \sin \phi) \sin \theta + z \cos \theta$$

$$\begin{aligned} \bar{a}_E = & -(\cos \phi \cos \theta \sin P + \sin \phi \cos P) \bar{a}_x \\ & -(\sin \phi \cos \theta \sin P - \cos \phi \cos P) \bar{a}_y \\ & + \sin \theta \sin P \bar{a}_z . \end{aligned}$$

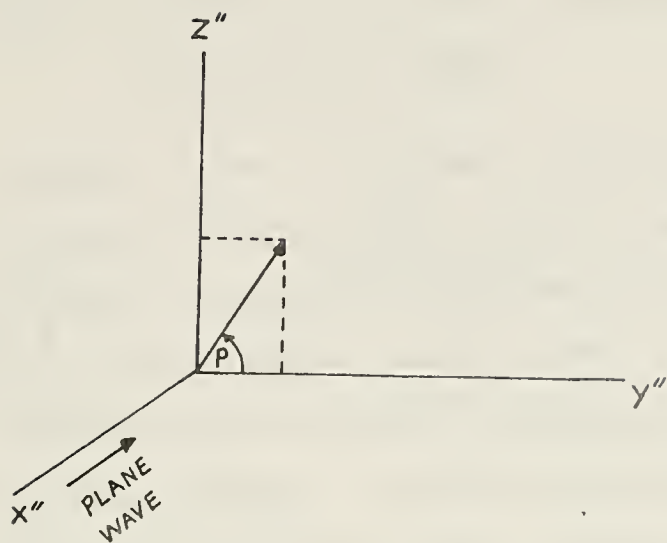


FIGURE 7. SPECIFICATION OF A PLANE WAVE.

IV. CALCULATION OF MUTUAL IMPEDANCE BETWEEN TWO FILAMENTARY DIPOLES WITH PIECEWISE SINUSOIDAL CURRENT DISTRIBUTION

The closed form formulas for mutual impedance between two filamentary dipoles with piecewise sinusoidal current distribution was published by King [13] and by Richmond and Geary [14,15]. When dipoles are far apart, the mutual impedance can be obtained efficiently by numerical integration. For closely coupled dipoles, a straight forward numerical integration cannot be used because of the singularity of the integrand. One way to overcome this problem is by removing the singularities. This method, suggested to the author by J.H. Richmond in personal communication is to be described here.

The mutual impedance between two dipoles can be obtained from the reaction between four pairs of monopoles. The relative position of two monopoles are defined in figure 8. (This arrangement is due to Richmond [4].) The length of each monopole must not exceed one quarter wavelength. Current distributions in monopole "a" and "b" are assumed to be:

$$\bar{I}^a(z) = \frac{I_1^a \text{sink}(z_2-z) + I_2^a \text{sink}(z-z_2)}{\text{sink}(z_2-z_1)} \bar{a}_z \quad (31)$$

$$\bar{I}^b(z') = \frac{I_1^b \text{sink}(z_2'-z') + I_2^b \text{sink}(z'-z_2')}{\text{sink}(z_2'-z_1')} \bar{a}_{z'} \quad (32)$$

The reaction between monopoles "a" and "b" is

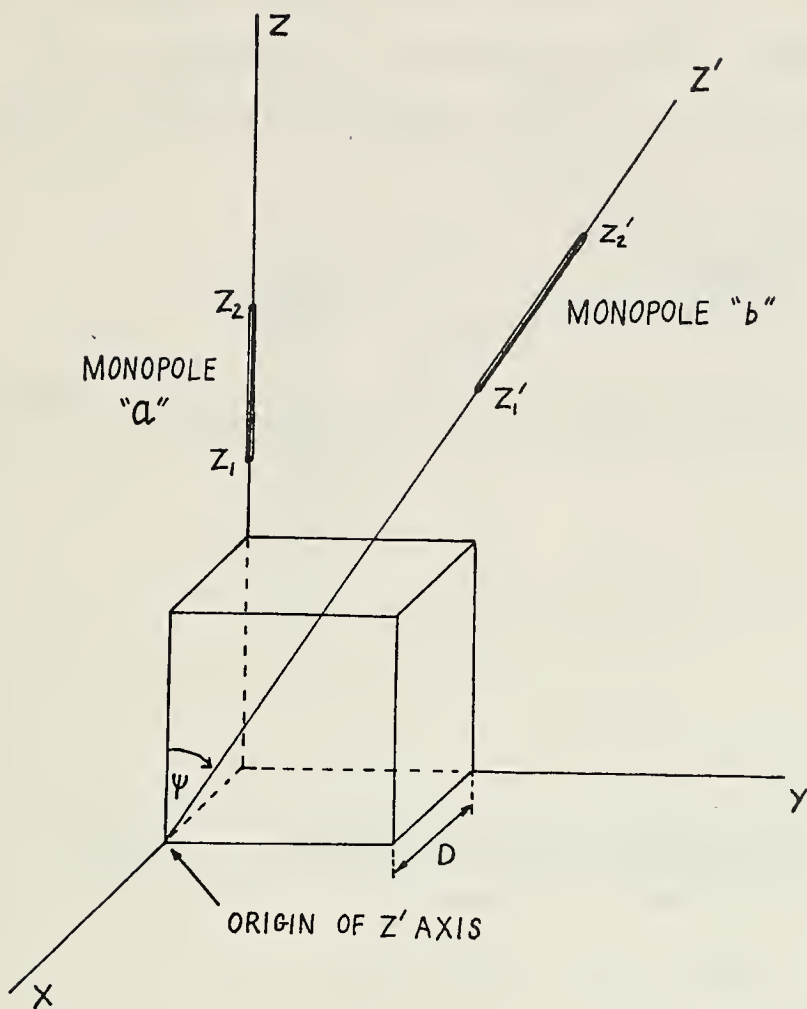


FIGURE 8. ARRANGEMENT OF TWO ARBITRARILY ORIENTED MONOPOLES.

$$\langle a, b \rangle = \int_{z_1'}^{z_2'} \bar{E}^a(z') \cdot \bar{I}^b(z') dz' \quad (33)$$

where $\bar{E}^a(z')$ is the electric field due to monopole "a" alone in the medium. The exact field of an electric line source with sinusoidal current distribution is known [17,18].

$$\bar{E}^a = E_z^a \bar{a}_z + E_\rho^a \bar{a}_\rho \quad (34)$$

$$E_z^a = \frac{k}{j4\pi\omega\epsilon \text{sink}(z_2 - z_1)} \sum_{n=1}^2 P_n \frac{e^{-jkR_n}}{R_n}$$

$$E_\rho^a = \frac{k}{j4\pi\omega\epsilon\rho \text{sink}(z_2' - z_1')} \sum_{n=1}^2 [-P_n \cos\theta_n + jS_n] e^{-jkR_n}$$

$$\text{where } P_1 = I_1^a \cos k(z_2 - z_1) + I_2^a$$

$$P_2 = I_1^a - I_2^a \cos k(z_2 - z_1)$$

$$S_1 = I_1^a \text{sink}(z_2 - z_1)$$

$$S_2 = -I_2^a \text{sink}(z_2 - z_1)$$

R_n and θ_n are defined in figure 9.

$\bar{I}^b(z')$ in (32) can be put in the form

$$\bar{I}^b(z') = \frac{Q \text{sink}(z' - z_m)}{\text{sink}(z_2' - z_1')} \bar{a}_{z'}, \quad (35)$$

where Q and z_m are constants. Substituting in (33) gives

$$\langle a, b \rangle = K \int_{z_1'}^{z_2'} \sum_{n=1}^2$$

$$\frac{(D^2 \cos\psi P_n + \sin^2\psi P_n z_n z' + jS_n \sin^2\psi z' R_n) e^{-jkR_n} \text{sink}(z' - z_m) dz}{(\sin^2\psi z'^2 + D^2) R_n} \quad (36)$$

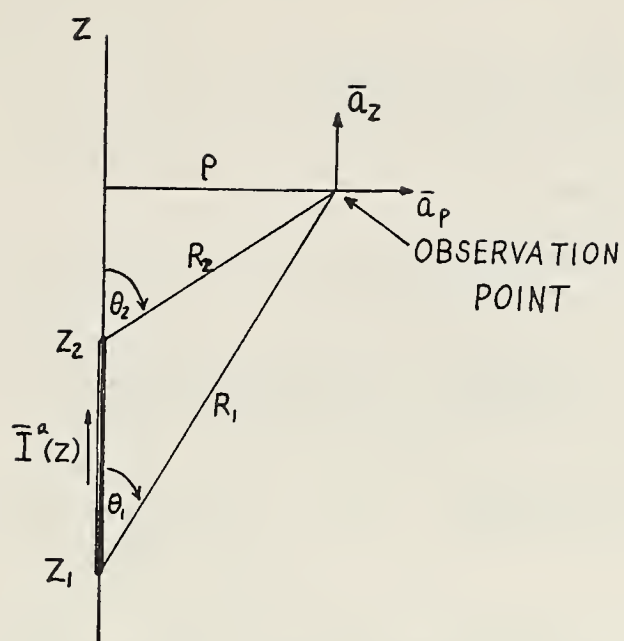


FIGURE 9. ELECTRIC FIELD OF MONOPOLE "a" .

$$\text{where } R_n = \sqrt{(z' - a_n)^2 + b_n^2}$$

$$a_n = z_n \cos \psi$$

$$b_n = \sqrt{z_n^2 \sin^2 \psi + D^2}$$

$$K = \frac{Q}{j4\pi \sin k(z_2 - z_1) \sin k(z'_2 - z'_1)} \sqrt{\frac{\mu}{\epsilon}}$$

For parallel monopoles $\sin \psi$ is equal to zero, and (36) reduces to

$$\langle a, b \rangle = K \int_{z'_1}^{z'_2} \sum_{n=1}^2 \frac{P_n e^{-jkR_n} \sin k(z' - z_m) dz'}{R_n} \quad (37)$$

For coplanar elements D is zero and (36) becomes

$$\langle a, b \rangle = K \int_{z'_1}^{z'_2} \sum_{n=1}^2 \frac{(P_n z_n + jS_n R_n) e^{-jkR_n} \sin k(z' - z_m) dz'}{R_n z'} \quad (38)$$

When the minimum separation distance between the monopoles is greater than 0.05λ , the mutual impedance can be efficiently calculated by numerical integration. To use numerical integration at close range, one has to employ special technique. One of the techniques that can be used is the singularity extraction method which involves removing the singularity from the integrand and adding their contribution back later in closed form. From numerical experiment, it was found that only the real part of integrand (or the imaginary

part of the mutual impedance) needs singularity extraction treatment. The formula with singularities extracted for the parallel case is

$$\begin{aligned} \langle a, b \rangle = & K \sum_{n=1}^2 P_n \int_{z'_1}^{z'_2} \frac{e^{-jkR_n} \text{sink}(z'-z_m) - \text{sink}(a_n - z_m)}{R_n} dz \\ & + \text{sink}(a_n - z_m) \ln(R_n + z' - a_n) \Big|_{z'_1}^{z'_2} \quad (39) \end{aligned}$$

For coplanar case, the formula is

$$\begin{aligned} \langle a, b \rangle = & K \sum_{n=1}^2 \left[\int_{z'_1}^{z'_2} \left\{ \frac{(P_n Z_n + j S_n R_n) e^{-jkR_n} \text{sink}(z' - z_m)}{R_n Z'} \right. \right. \\ & \left. \left. - \frac{H_{0n} + H_{1n} Z'}{R_n Z'} \right\} dz' \right. \\ & \left. + \frac{H_{0n}}{C_n} \ln \frac{R_n + Z' - C_n}{R_n + Z' + C_n} \Big|_{z'_1}^{z'_2} + H_{1n} \ln(R_n + z' - a_n) \Big|_{z'_1}^{z'_2} \right] \quad (40) \end{aligned}$$

where $H_{0n} = (P_n Z_n \cos k c_n + S_n c_n \text{sink } c_n) \text{sink}(-z_m)$

$H_{1n} = \frac{P_n Z_n}{C_n} \text{sink } c_n - S_n \cos k c_n \cos k z_m$

and $C_n = \sqrt{a_n^2 + b_n^2}$.

For the general case the formula is

$$\begin{aligned} \langle a, b \rangle = & K \sum_{n=1}^2 \left[\int_{z'_1}^{z'_2} \left\{ \frac{(P_n d^2 \cos \psi + P_n Z_n z' + j S_n z' R_n) e^{-jkR_n} \text{sink}(z' - z_m)}{(z'^2 + d^2) R_n} \right. \right. \\ & \left. \left. - \frac{G_{0n} + G_{1n} z' + G_{2n} z' R_n}{z'^2 + d^2} \right\} dz' \right. \\ & \left. - \frac{G_{0n}}{d} \text{Im } T_n + G_{1n} \text{Re } T_n + G_{2n} \ln(R_n + z' - a_n) \Big|_{z'_1}^{z'_2} \right] \quad (41) \end{aligned}$$

where $d = \frac{D}{\sin \psi}$

$$G_{on} = d \operatorname{Im} U_n$$

$$G_{ln} = \operatorname{Re} U_n$$

$$U_n = (P_n(Z_n + jd \cos \psi) \cos kc'_n + S_n c'_n \sin kc'_n) \sin(-jd - z_m)$$

$$G_{zn} = \operatorname{Re} \left[\frac{P_n(Z_n + jd \cos \psi) \sin kc'_n}{c'_n} - S_n \cos kc'_n \right] \cos(-jd - z_m)$$

$$T_n = \frac{1}{c'_n} \ln \frac{R_n + z'_1 + jd - c'_n}{R_n + z'_1 + jd + c'_n} \Big|_{z'_1}^{z'_2}$$

$$c'_n = Z_n + jD \cot \psi .$$

The principle value of the logarithm of complex number is to be used when T_n is computed. Equation (41) fails when monopoles are parallel. A computer program was written based on equations (39) and (41).

Results obtained from the singularity extraction method are compared against those obtained from closed form method and the ordinary numerical integration method in table 2. When the four-point Gaussian quadrature formula is used, the singularity extraction method is at least four times faster than that of the closed form method, while the results agree well with the closed form solution as seen in table 2.

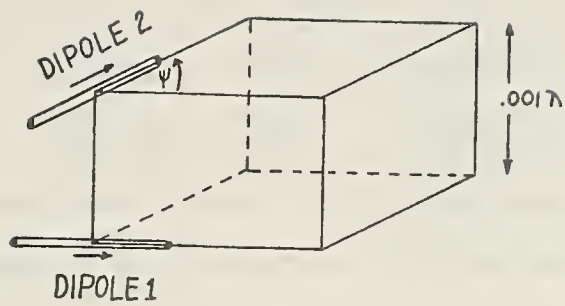


FIGURE 10. DIPOLE CONFIGURATION FOR TABLE 2.

Both dipoles are symmetrically driven. The assumed current is piecewise sinusoidal.

TABLE 2. MUTUAL IMPEDANCE BETWEEN DIPOLES IN FIGURE 10 BY
THREE METHODS.

mutual impedance in ohms			
ψ , degrees	method 1.	method 2	method 3
0.0	8.334 -j588.628	8.334 -j586.503	8.334-j395.4
15.0	8.050 -j193.682	8.050 -j193.700	8.050+j 45.4
30.0	7.217 -j106.510	7.217 -j106.505	7.217+j 83.2
45.0	5.893 -j62.859	5.892 -j 62.859	8.893+j 70.9
60.0	4.166 -j35.769	4.167 -j 35.553	4.167+j 49.3
75.0	2.157 -j16.309	2.156 -j16.189	2.157+j 25.1
90.0	0.000 +j 0.002	0.000 +j 0.000	0.000+j 0.001

method 1: Closed form method programmed by Richmond [4].

method 2: Numerical integration method with singularities extracted, four point Gaussian quadrature formula.

method 3: Numerical integration method, four point Gaussian quadrature formula.

V. NUMERICAL RESULTS

A computer program was written to solve for surface current distribution induced on conducting bodies of arbitrary shapes due to an incident plane wave. The surface of the conducting body is defined by interconnecting rectangular or near-rectangular patches. Two directions of current were assumed for each patch. The magnetic field intensity of the plane wave at the origin was one ampere/meter and zero phase. All elements of the matrix were calculated.

A. A RECTANGULAR PLATE

The conducting body is a rectangular plate of negligible thickness shown in figure 11. The plate was divided into 32 square patches. The results are shown in figure 12 and table 3. In this problem both \bar{J}_z and \bar{J}_y have singularities at the edges, but they are approximated by finite current when the method described in this thesis is applied.

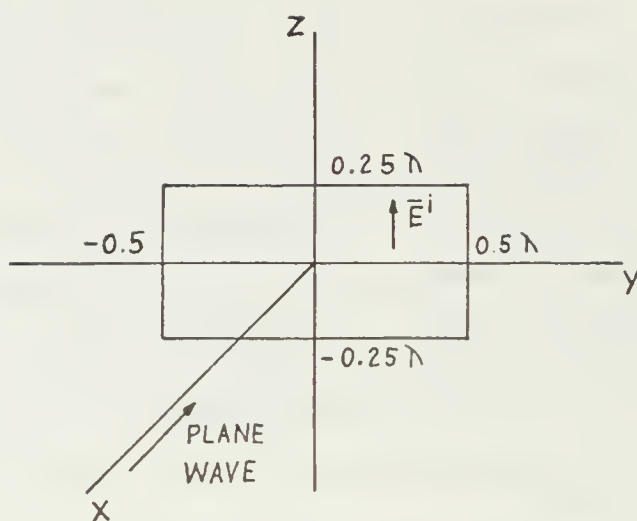


FIGURE 11. DESCRIPTION OF RECTANGULAR PLATE PROBLEM.

TABLE 3. CURRENT ON RECTANGULAR PLATE OF FIGURE 11.

a. $|\bar{J}_z(y,z)|$, amp/meter

0.25	0.0	0.0	0.0	0.0	0.0	0.0	0.0	0.0	0.0
0.125	7.55	3.45	4.43	3.29	2.82	3.29	4.43	3.45	7.55
0.0	11.68	4.30	3.51	3.78	5.40	3.78	3.51	4.30	11.68
-0.125	7.55	3.45	4.43	3.29	2.82	3.29	4.43	3.45	7.55
0.25	0.0	0.0	0.0	0.0	0.0	0.0	0.0	0.0	0.0
$z \uparrow \vec{y}$	-0.5	-0.375	-0.25	-0.125	0.0	0.125	0.25	0.375	0.5

b. $|\bar{J}_y(y,z)|$, amp/meter

0.25	0.0	2.10	2.21	3.42	0.0	3.42	2.21	2.10	0.0
0.125	0.0	1.95	0.44	1.78	0.0	1.78	0.44	1.95	0.0
0.0	0.0	0.0	0.0	0.0	0.0	0.0	0.0	0.0	0.0
-0.125	0.0	1.45	0.44	1.78	0.0	1.78	0.44	1.95	0.0
-0.25	0.0	2.10	2.21	3.42	0.0	3.42	2.21	2.10	0.0
$z \uparrow \vec{y}$	-0.5	-0.375	-0.25	-0.125	0.0	0.125	0.25	0.375	0.5

FIGURE 12. THE ISOMETRIC PLOT OF CURRENT ON THE RECTANGULAR
PLATE OF FIGURE 11,

(a) $|\bar{J}_z|$

(b) $|\bar{J}_y|$.

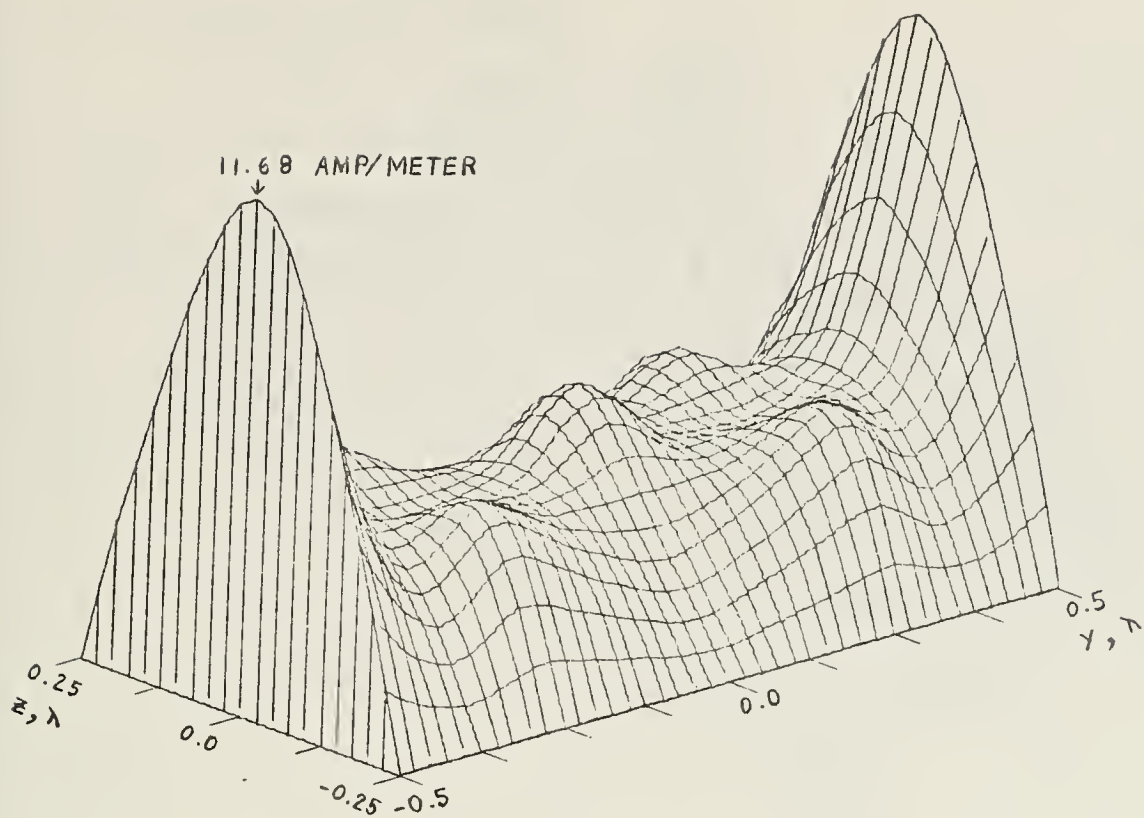


FIGURE 12A.

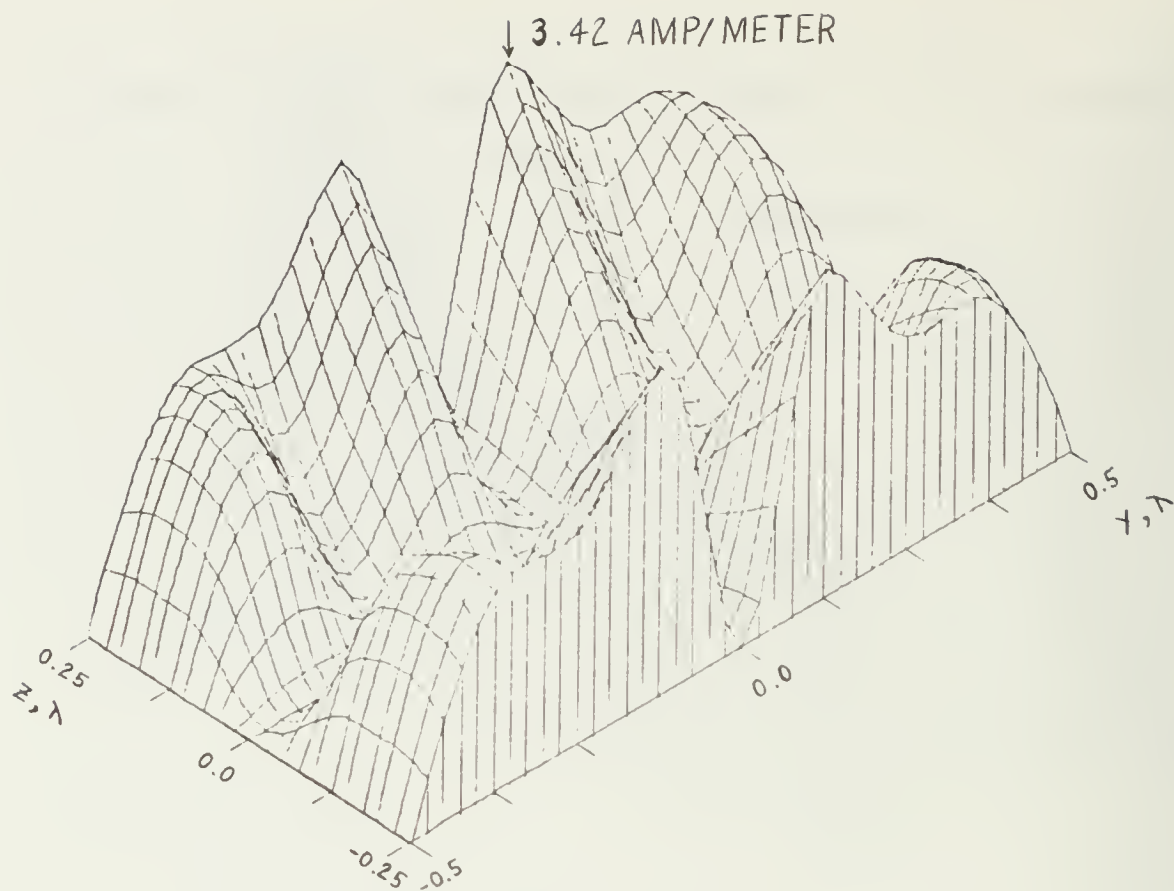


FIGURE 12B.

B. SQUARE PLATE PROBLEM

The conducting body is a square plate shown in figure 13. In part one, the plane wave comes from the direction $\phi = 0$ and $\theta = 90$ degrees; in part two, from $\phi = 45$, $\theta = 90$ degrees; and in part three, from $\phi = 0$, $\theta = 45$ degrees.

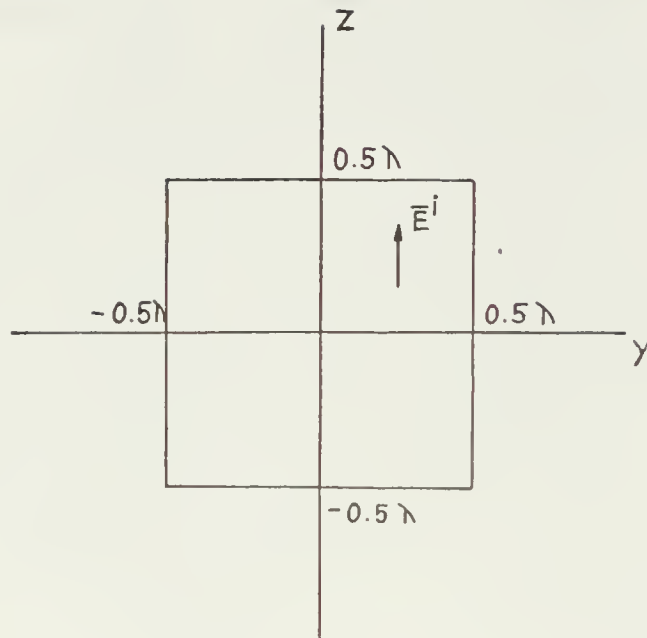


FIGURE 13. DESCRIPTION OF SQUARE PLATE PROBLEM.

Table 4. CURRENT ON SQUARE PLATE OF FIGURE 13 FOR BROAD-SIDE INCIDENCE.

a. $|\bar{J}_z(x, z)|$, amp/meter

0.5	0.0	0.0	0.0	0.0	0.0	0.0	0.0	0.0	0.0
0.375	1.73	1.14	1.41	1.38	1.61	1.38	1.41	1.14	1.73
0.25	4.23	1.33	1.81	1.77	1.95	1.77	1.81	1.33	4.23
0.125	6.53	1.75	2.42	2.29	2.52	2.29	2.42	1.75	6.53
0.0	7.44	2.04	2.70	2.44	2.74	2.44	2.70	2.04	7.44
-0.125	6.53	1.75	2.42	2.29	2.52	2.29	2.42	1.75	6.53
0.25	4.23	1.33	1.81	1.77	1.95	1.77	1.81	1.33	4.23
-0.375	1.73	1.14	1.41	1.38	1.61	1.38	1.41	1.14	1.73
0.5	0.0	0.0	0.0	0.0	0.0	0.0	0.0	0.0	0.0
$\begin{matrix} \uparrow \\ z \end{matrix} \begin{matrix} \rightarrow \\ y \end{matrix}$	-0.5	-0.375	-0.25	-0.125	0.0	0.125	0.25	0.375	0.5

Table 4. con't

b. $|\bar{J}_y(\cdot, z)|$, amp/meter

0.5	0.0	0.32	0.64	0.37	0.0	0.37	0.64	0.32	0.0
0.375	0.0	0.16	0.30	0.17	0.0	0.17	0.30	0.16	0.0
0.25	0.0	0.08	0.14	0.10	0.0	0.10	0.14	0.08	0.0
0.125	0.0	0.11	0.06	0.13	0.0	0.13	0.06	0.11	0.0
0.0	0.0	0.0	0.0	0.0	0.0	0.0	0.0	0.0	0.0
-0.125	0.0	0.11	0.06	0.13	0.0	0.13	0.06	0.11	0.0
-0.25	0.0	0.08	0.14	0.10	0.0	0.10	0.14	0.08	0.0
-0.375	0.0	0.17	0.30	0.17	0.0	0.17	0.30	0.17	0.0
-0.5	0.0	0.32	0.64	0.37	0.0	0.37	0.64	0.32	0.0
$z \uparrow \vec{y}$	-0.5	-0.375	-0.25	-0.125	0.0	0.125	0.25	0.375	0.5

Figure 14. THE ISOMETRIC PLOT OF CURRENT ON THE SQUARE
PLATE OF FIGURE 13.

14.1 Broadside incidence

(a) $|\bar{J}_z(y,z)|$

(b) $|\bar{J}_y(y,z)|$

14.2 $\phi = 45^\circ$, $\theta = 90^\circ$ degrees

(a) $|\bar{J}_z(y,z)|$, $J_{\max} = 8.52$ amp/meter

(b) $|\bar{J}_y(y,z)|$, $J_{\max} = 4.72$ amp/meter

14.3 $\phi = 0^\circ$, $\theta = 45^\circ$ degrees

(a) $|\bar{J}_z(y,z)|$, $J_{\max} = 10.82$ amp/meter

(b) $|\bar{J}_y(y,z)|$, $J_{\max} = 3.86$ amp/meter

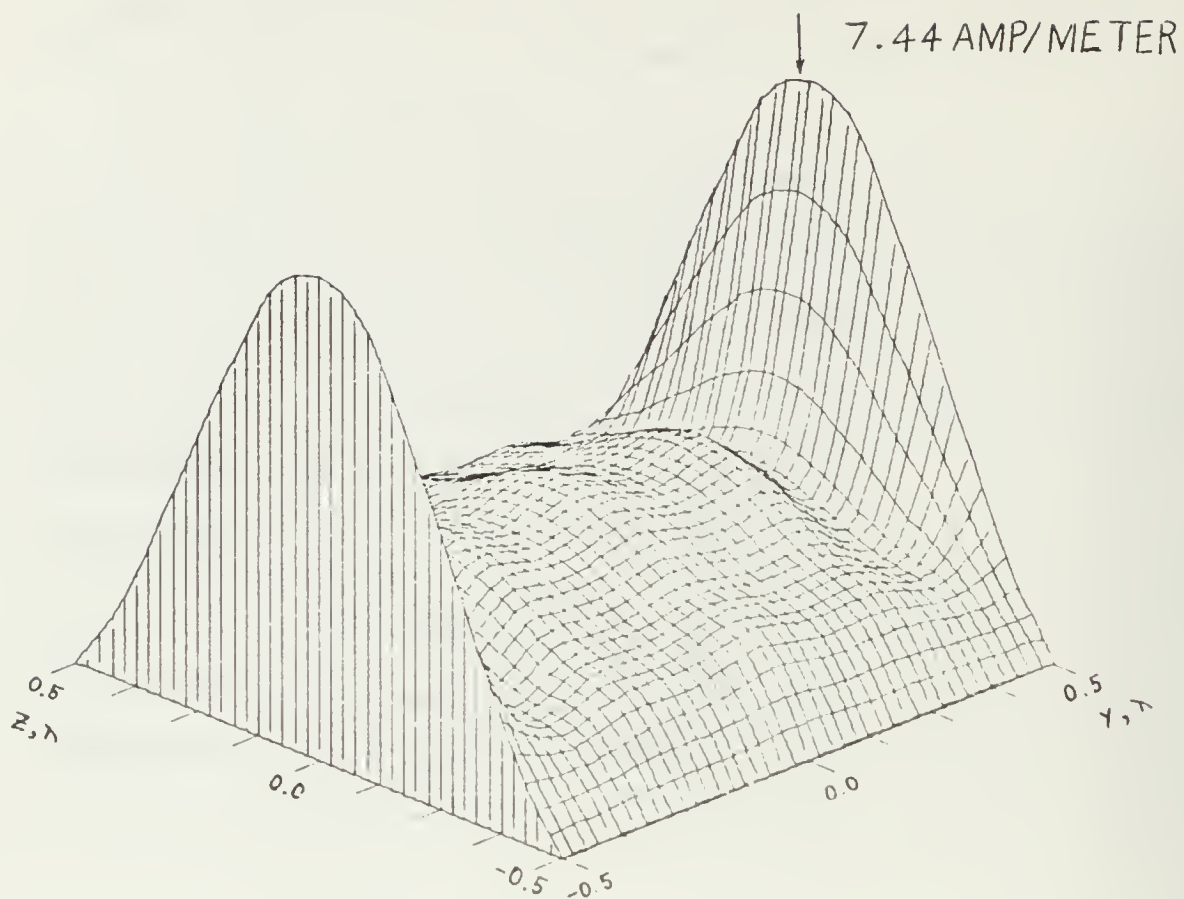


FIGURE 14.1A.

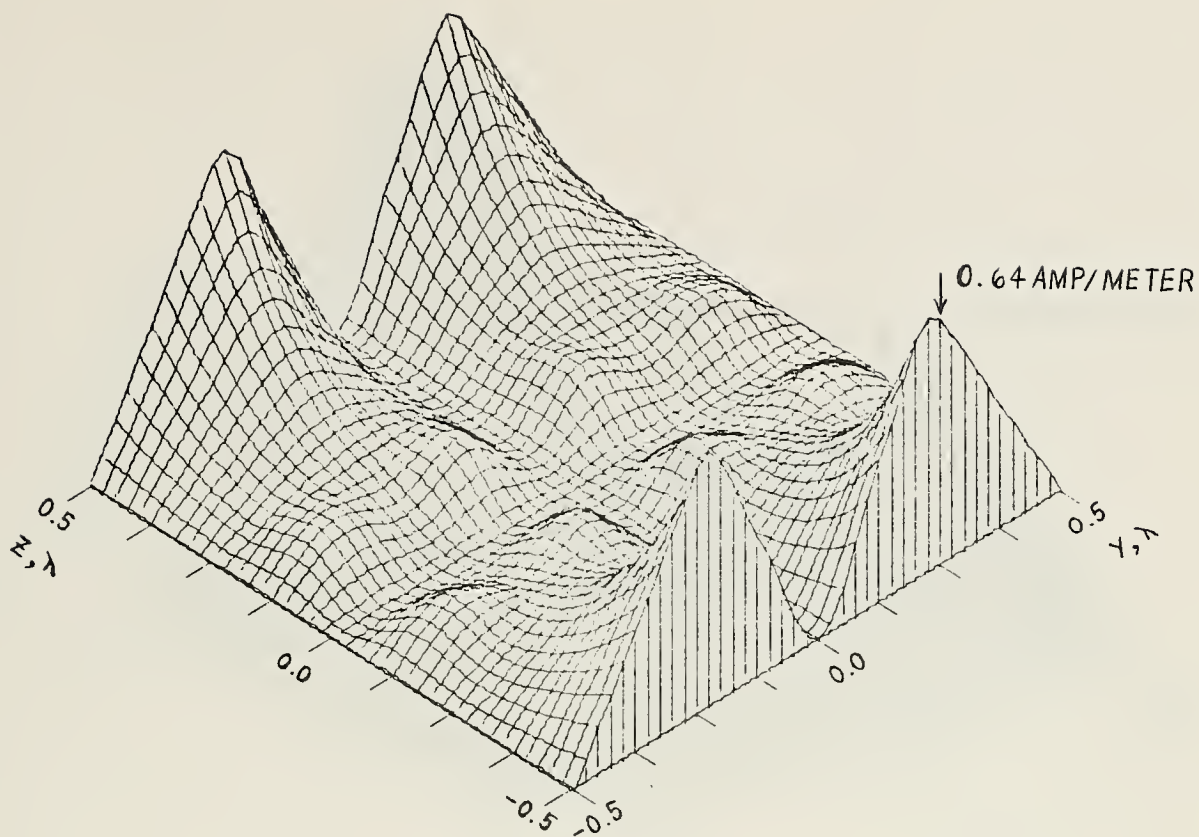


FIGURE 14.1B.

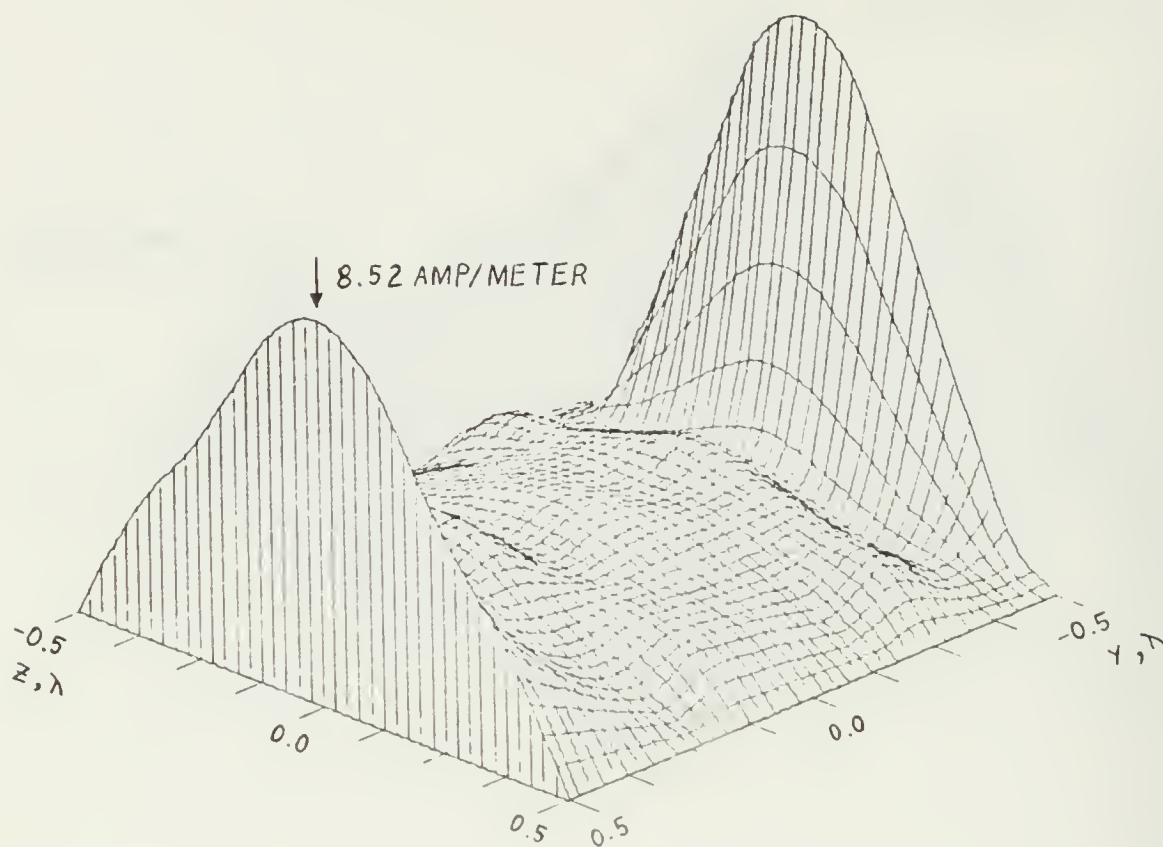


FIGURE 14.2A.

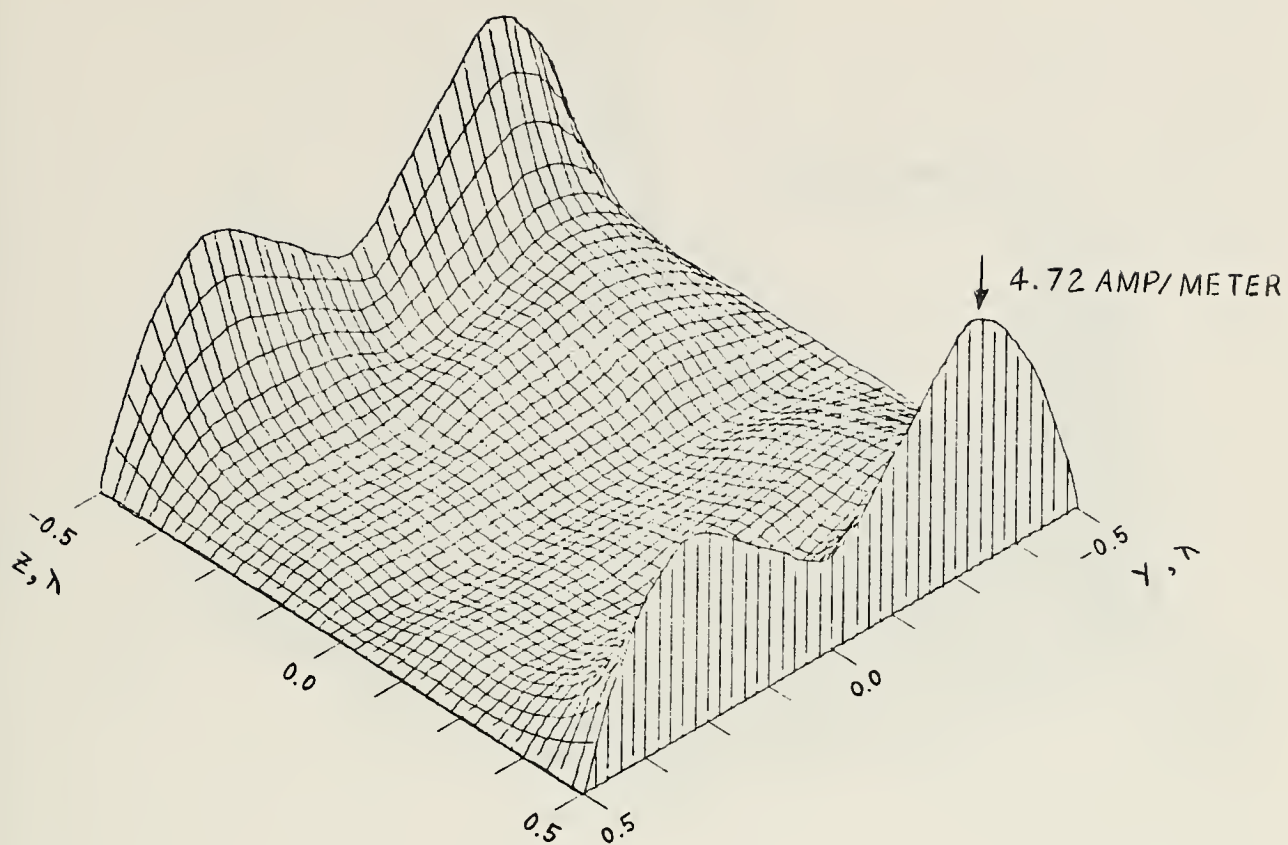


FIGURE 14.2B.

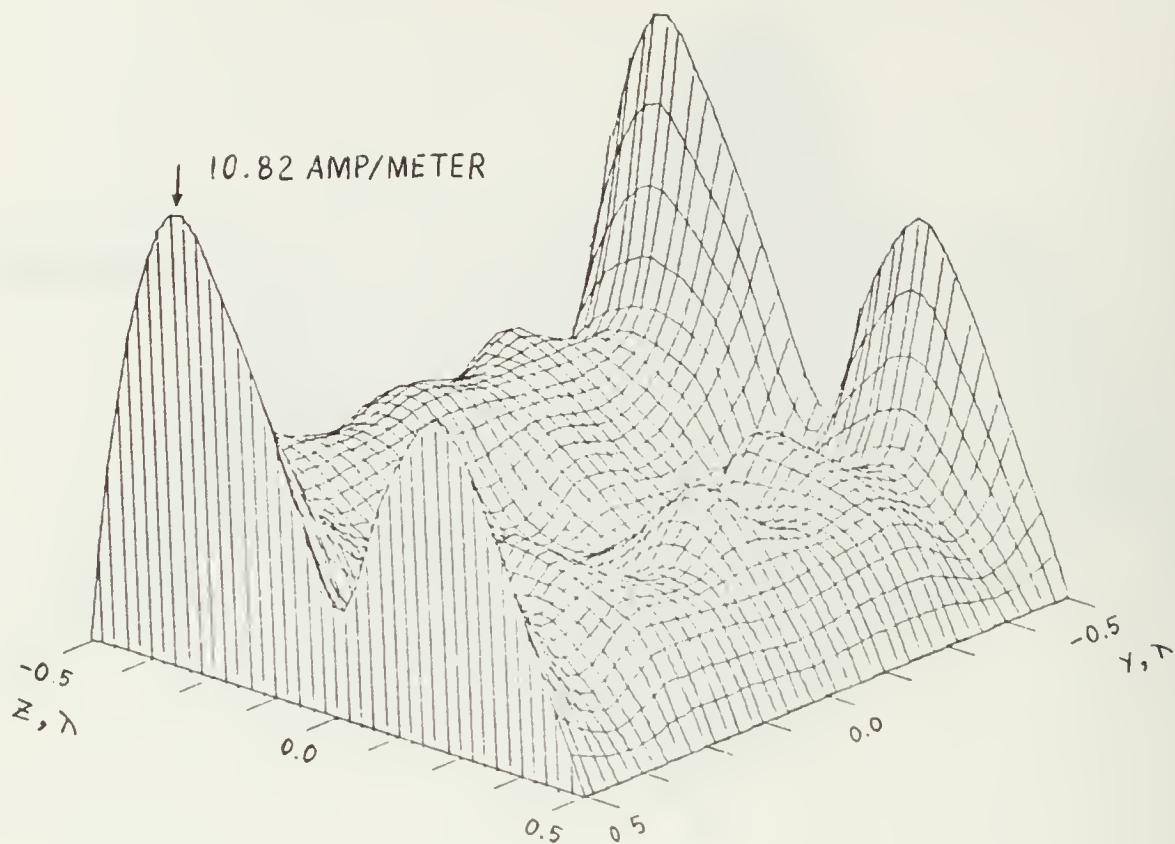


FIGURE 14.3A.

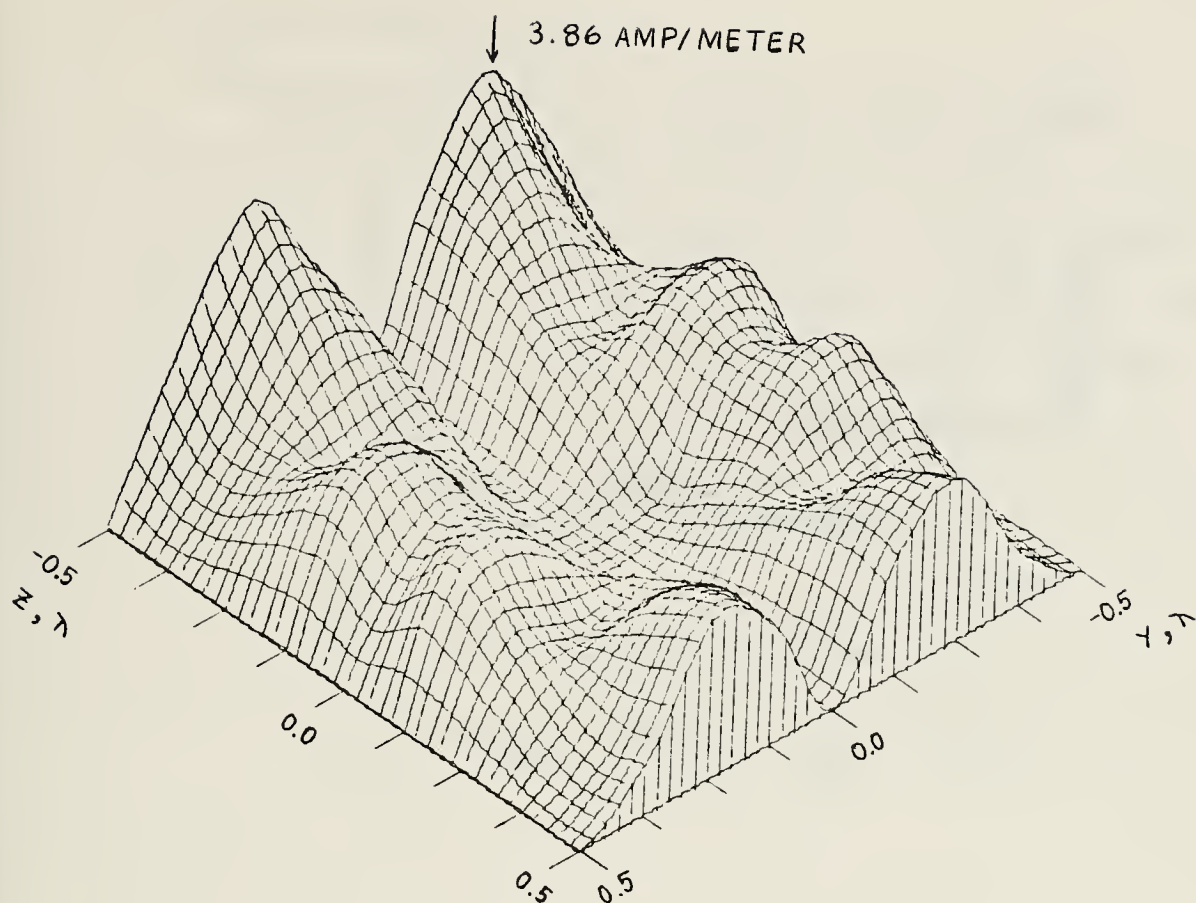


FIGURE 14.3B.

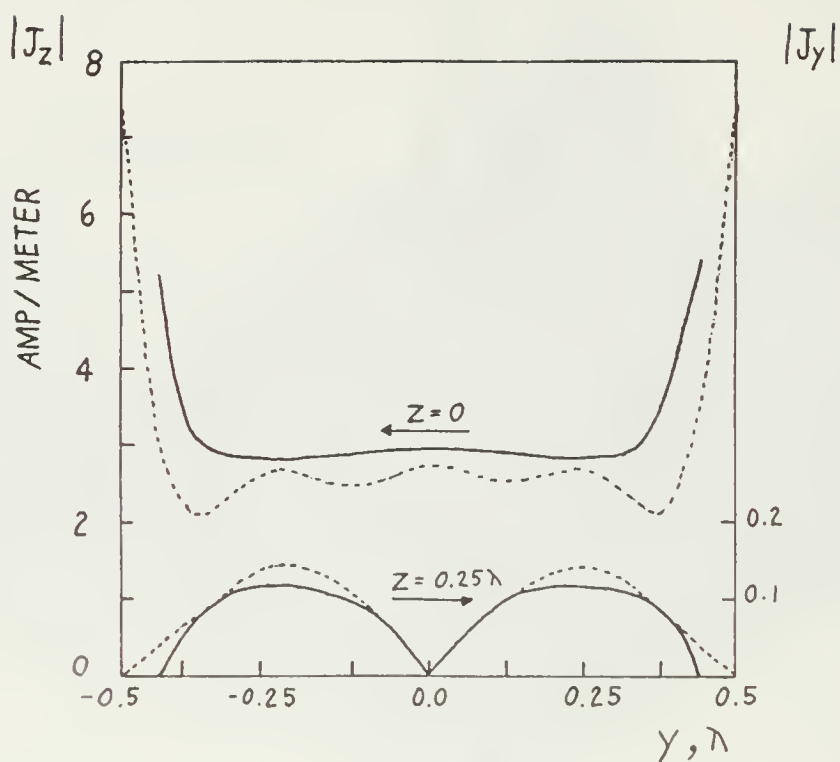


FIGURE 15. CURRENTS ON SQUARE PLATE FOR BROADSIDE
INCIDENCE COMPARED WITH THOSE CALCULATED
BY RAMAT-SAMII AND MITTRA [10] (solid curve).

C. HOLLOW CYLINDRICAL TUBE

The conducting body is a hollow cylindrical tube of finite length and octagonal cross section shown in figure 16. The results compared with the theoretical and experimental results obtained by Kao [18] for a hollow cylindrical tube with circular cross section is not in complete agreement. Differences shown may be due to the approximation of a curved surface by flat surfaces.

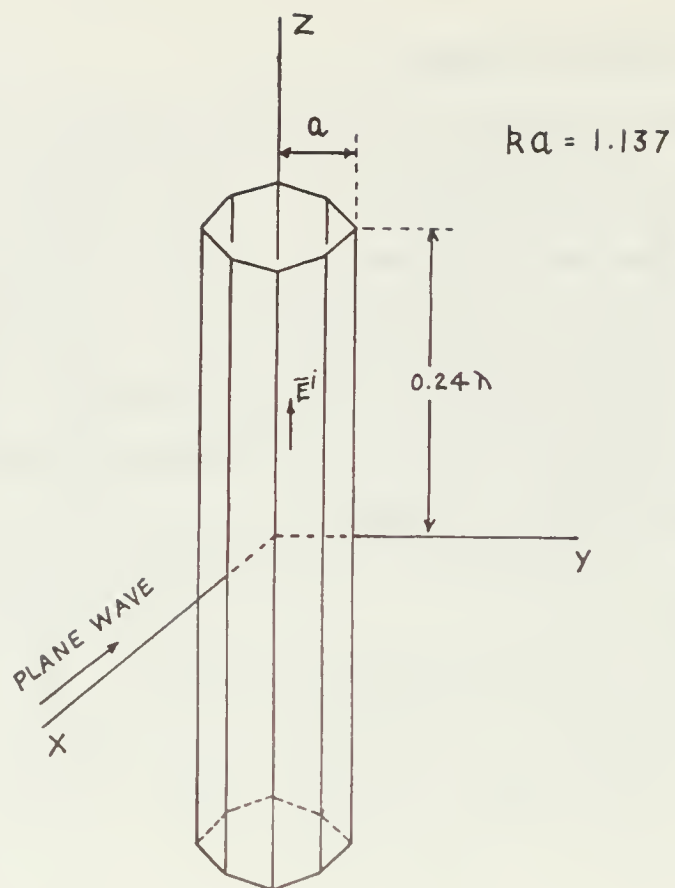


FIGURE 16. DESCRIPTION OF HOLLOW CYLINDRICAL TUBE PROBLEM.

FIGURE 17. THE ISOMETRIC PLOT OF CURRENT ON HOLLOW
CYLINDRICAL TUBE OF FIGURE 16.

- (a) $|\bar{J}_z(z, \phi)|$, $J_{\max} = 3.08$ amp/meter
(b) $|\bar{J}(z, \phi)|$, $J_{\max} = 7.69$ amp/meter

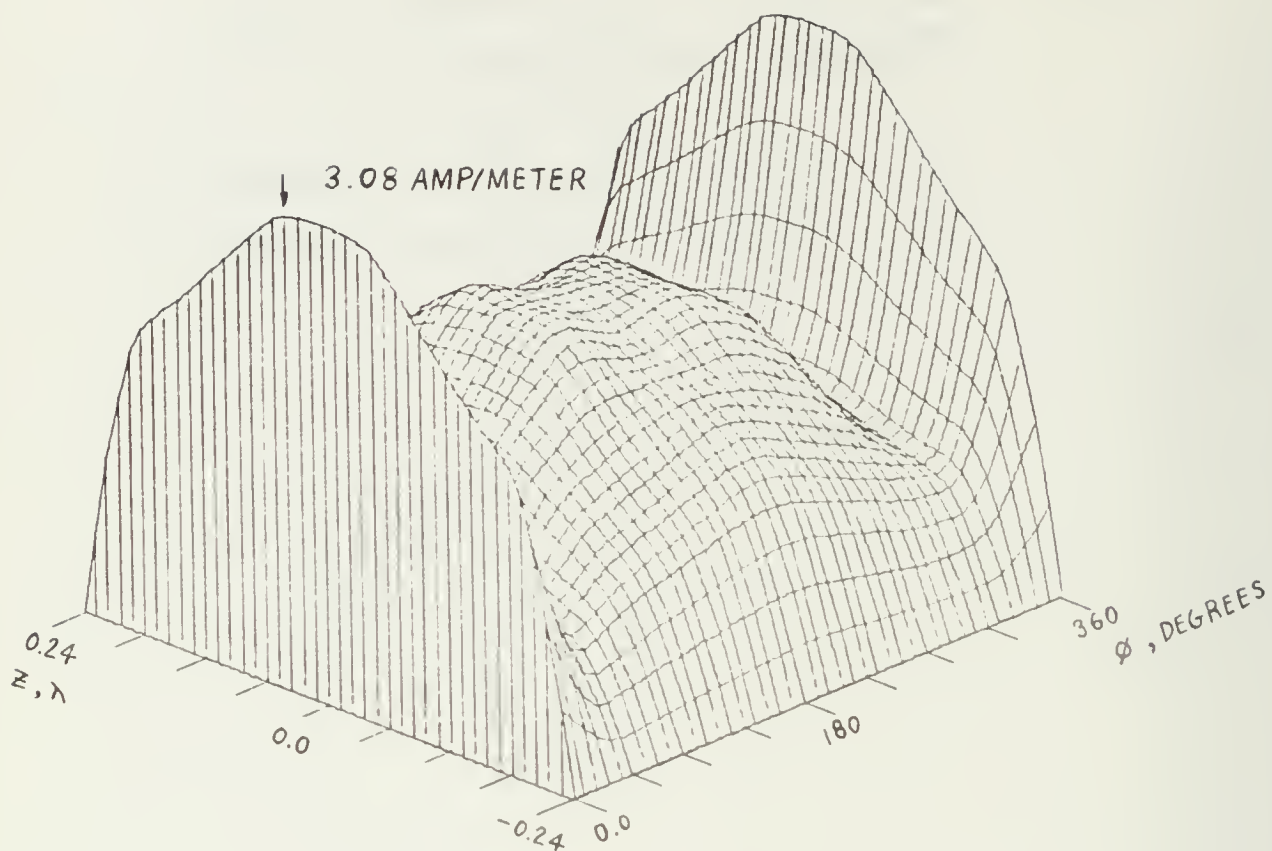


FIGURE 17A

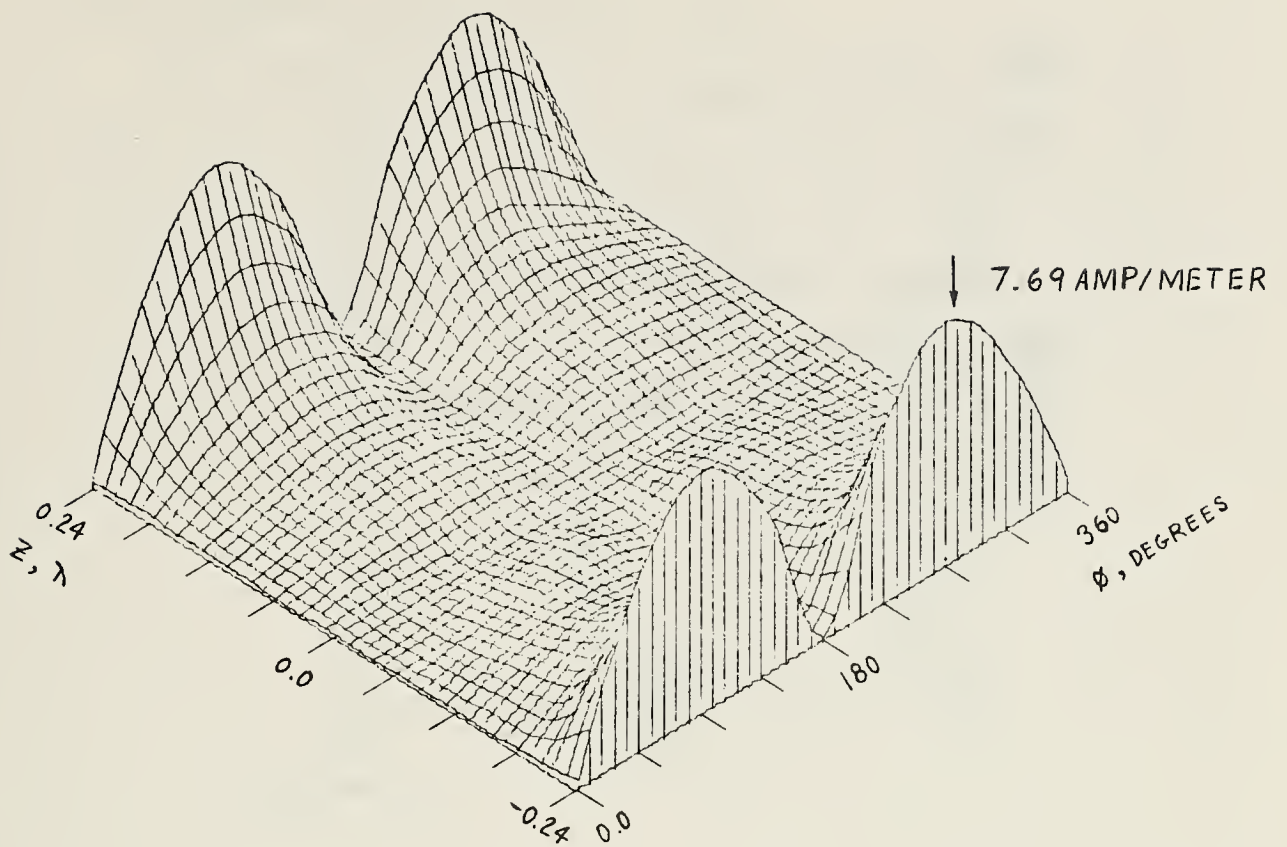


FIGURE 17B.

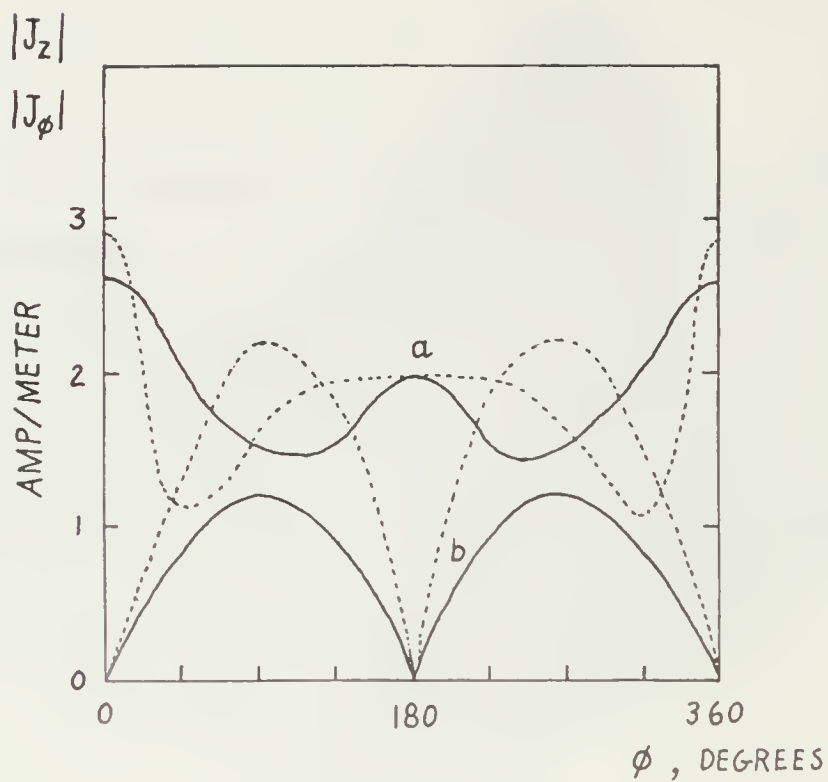


FIGURE 18. CURRENTS ON HOLLOW CYLINDRICAL TUBE COMPARED WITH THOSE CALCULATED BY KAO [18] FOR THE SAME GEOMETRY BUT WITH CIRCULAR CROSS SECTION. (Kao-solid curve).

(a) $|\bar{J}_z|$ at $z=0$

(b) $|\bar{J}_\phi|$ at $z=0.18\lambda$

D. L-SHAPED HOLLOW CYLINDRICAL TUBE

The conducting body is an L-shaped hollow cylindrical tube with octagonal cross section shown in figure 19. The plane wave comes from the direction $\phi = 0$ and $\theta = 90$ degrees. In this problem, non-rectangular patches were used at the corners. The current distribution were plotted as if the tube were straight.

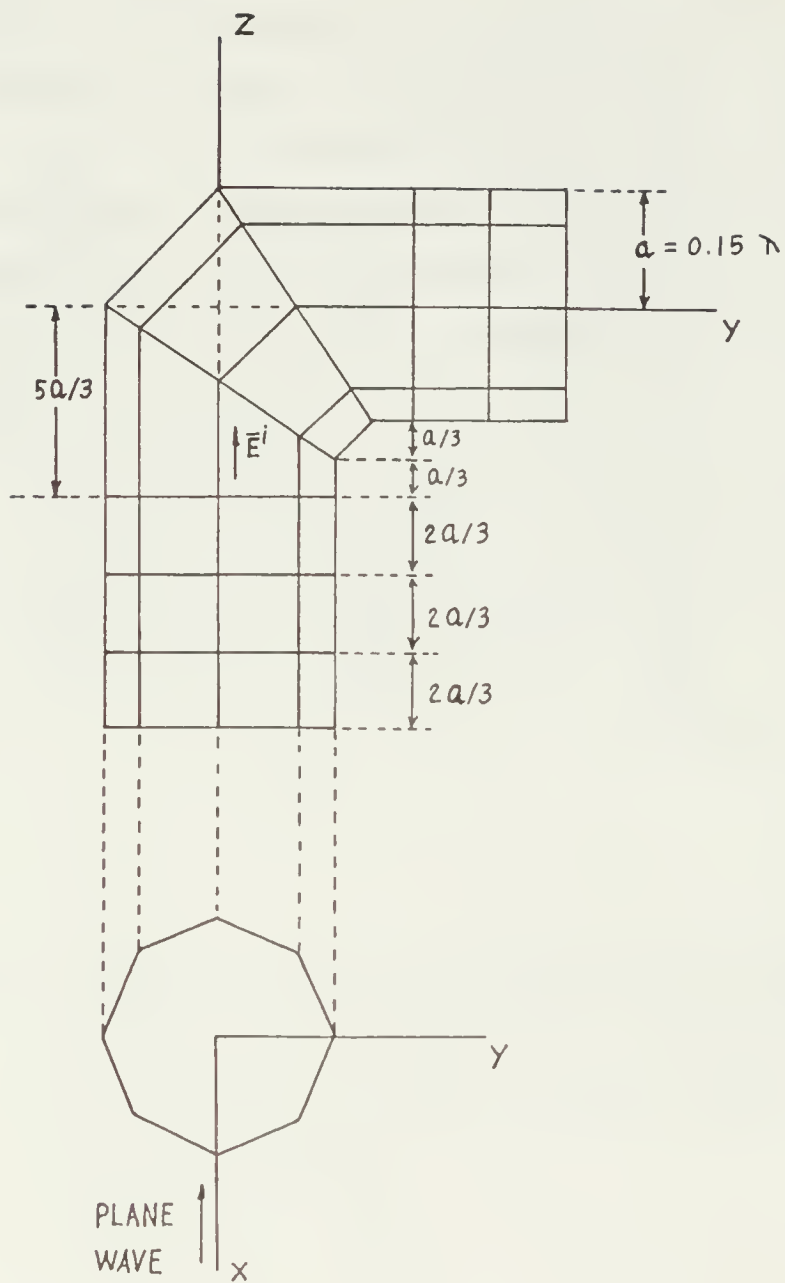


FIGURE 19. DESCRIPTION OF L-SHAPED HOLLOW CYLINDRICAL TUBE.

FIGURE 20. THE ISOMETRIC PLOT OF CURRENT ON L-SHAPED
HOLLOW CYLINDRICAL TUBE OF FIGURE 19,

(a) axial component, $J_{\max} = 3.08$ amp/meter

(b) circumferential component, $J_{\max} = 5.14$
amp/meter.

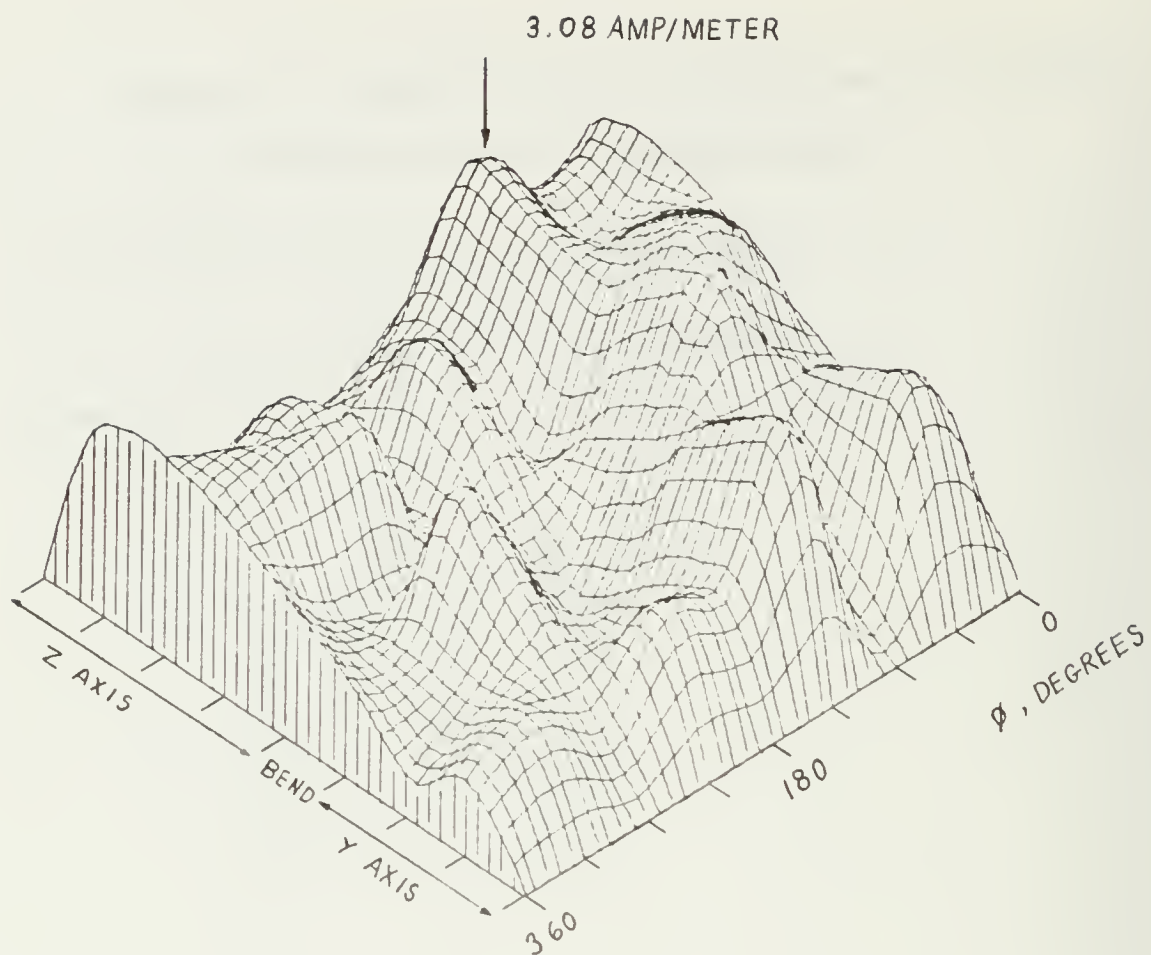


FIGURE 20A.

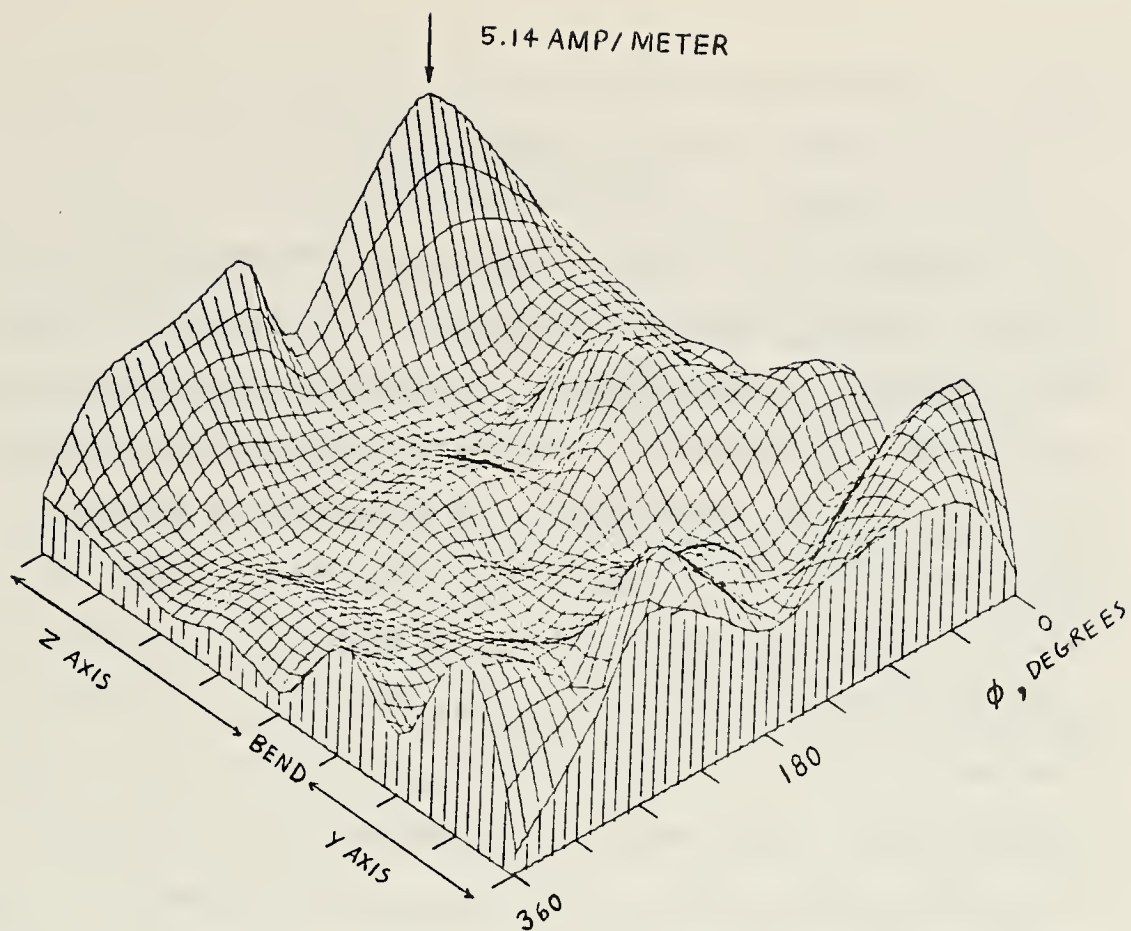


FIGURE 20B.

VI. CONCLUSIONS

A method to calculate current induced on perfectly conducting bodies of arbitrary shape due to impressed fields was presented in this thesis. The approach was based mathematically on the method of moments and physically on the reaction matching technique. The bases chosen were two dimensional piecewise sinusoidal functions, so that the actual current can be closely approximated. Galerkin's method was used to form the linear equations to assure that the matrix to be inverted would be well conditioned. The simplicity of point matching and constant current patches was sacrificed for the advantage of the PSRMT method, namely rapid convergence, and useable results with relatively large sized patches. Preliminary results indicated that this method gives useful answers with the patches as large as 0.25λ by 0.25λ in dimension.

The solution time is essentially the time required to compute the coupling terms. Since the coupling terms were derived from the mutual impedance between piecewise sinusoidal line sources, it is very important to have a rapid mutual impedance subprogram. Formulas to calculate the mutual impedance by numerical integration with singularities extracted were presented. This method is at least four times faster than the closed form method, and the results agree well with

the closed form solution for the minimum separation of 0.001λ or greater. The time required to do the problem could be reduced greatly if symmetries were used. Symmetry considerations were discussed by Knorr [19]. In a practical program, reflection, translation and rotation symmetries should be used. No such feature was incorporated in the program written for this thesis.

From the solutions of problems solved in this thesis, it is clear that two directions of current are needed to approximate the current accurately, unless the quantities of interest are in the far field region, such as for a scattering cross section calculation.

The potential usefulness of this method as demonstrated warrants further investigation into its application as an engineering tool for solution of aircraft, vehicle, and ship problems.

A general purpose computer program for electromagnetic problems with two dimensional current distribution should have the following features:

- (1) The surface can be arbitrarily specified by the user, and a geometry generation subprogram is included so that finer division of the surface can be done automatically.

- (2) Plane of symmetry, axis of symmetry (for rotational symmetry), and line of symmetry (for translational symmetry) can be specified by the user; and symmetrical features are

used in the program to reduce the size of the matrix.

(3) The impressed fields and/or sources can be arbitrarily specified.

(4) The outputs consist of the current distribution, echo areas, near fields, etc.

Further theoretical investigations are needed in the following areas:

(1) A method of interfacing triangular patches with rectangular patches.

(2) A method of introducing local field excitation by a source attached to the surface.

LIST OF REFERENCES

1. Harrington, R.F., "Matrix Methods for Field Problems," Proc. IEEE, V.55, pp.136-149, February, 1967.
2. Harrington, R.F., Field Computation by Moment Methods, The McMillan Company, 1968.
3. Richmond, J.H., Radiation and Scattering by Thin-Wire Structures in the Complex Frequency Domain, National Aeronautic and Space Administration Contractor Report 2396. May, 1974.
4. Richmond, J.H., Computer Program for Thin-Wire Structures in a Homogeneous Conducting Medium, NASA CR-2399, June, 1974.
5. Richmond, J.H., "A Wire Grid Model for Scattering by Conducting Bodies," IEEE Trans. on Ant. and Prop., V.14, pp. 783-6.
6. Richmond, J.H. Wang, N., Sinusoidal Reaction Formulation for Radiation and Scattering from Conducting Surfaces, NASA CR-2398, June, 1974.
7. Harrington, R.F., Time-Harmonic Electromagnetic Fields, McGraw-Hill, Inc., 1961.
8. Rumsey, V.H., "Reaction Concept in Electromagnetic Theory," Physical Review, Vol. 94, June, 1954, pp. 1483-1491.
9. Tsai, L.L., Dudley, D.G., Wilton, D.R., "Electromagnetic Scattering by a Three-Dimensional Conducting Rectangular Box," Journal of Applied Physics, Vol.45, No.10, October 1974, pp.4393-4400.
10. Rahmat-Samii, Y., Mittra, R., "Integral Equation Solution and RSC Computation of a Thin Rectangular Plate," IEEE Trans. on Ant. and Prop., Vol. AP-22, No.4, July, 1974, pp. 608-610.
11. Scarborough, J.B., Numerical Mathematical Analysis, The John Hopkins Press, Baltimore, 6th ed., 1966, pp. 133-182.
12. Abramowitz, M., and Stegun, I.A., Handbook of Mathematical Functions with Formulas, Graphs, and Mathematical Tables, Dover Publication, New York, November 1970, Chapter 25.

13. King, H.E., "Mutual Impedance of Unequal Length Antennas in Echelon," IRE Trans. Antennas and Propagation, Vol. AP-5, July, 1957, pp. 306-313.
14. Richmond, J.H., Geary, N.H., "Mutual Impedance Between Co-Planar -- Skew Dipoles," IEEE Trans. on Ant. and Prop., Vol. AP-18, No. 3, May, 1970, pp.414-416.
15. Richmond, J.H., Geary, H.H., "Mutual Impedance of Non-planar - Skew Sinusoidal Dipoles," Report 2902-18, August, 1974, The Ohio State University ElectroScience Laboratory, Department of Electrical Engineering.
16. Schelkunoff, S.A., Friis, H.T., Antennas Theory and Practice, Wiley, New York, 1952, pp. 370-401.
17. Otto, D.V., Richmond, J.H., "Rigorous Field Expressions for Piecewise-Sinusoidal Line Sources," IEEE Trans. on Ant. and Prop., Jan, 1969, p. 98.
18. Kao, C.C., "Three Dimensional Electromagnetic Scattering from a Circular Tube of Finite Length," Journal of Applied Physics, Vol. 40, No. 12, November, 1969, pp. 4732-4740.
19. Knorr, J.B., "Consequences of Symmetry in the Computation of Characteristic Modes for Conducting Bodies," IEEE Trans. Ant. and Prop., Vol. AP-21, No. 6, November, 1973, pp. 899-902.

INITIAL DISTRIBUTION LIST

	No. Copies
1. Defense Documentation Center Cameron Station Alexandria, Virginia 22314	2
2. Library, Code 0212 Naval Postgraduate School Monterey, California 93940	2
3. Asst. Professor Richard W. Adler, Code 52Ab Department of Electrical Engineering Naval Postgraduate School Monterey, California 93940	5
4. 1Lt. Kharavuth Khemayodhin 193 North Rajsrirama Road, Dusit Bangkok 3, Thailand	1
5. Dr. J.H. Richmond ElectroScience Laboratory Ohio State University 1320 Kinnear Road Columbus, Ohio 43212	1
6. Dr. C.M. Butler University of Mississippi School of Electrical Engineering University, Mississippi 38677	1
7. Lt. Col. Albert Cupka Chief ELA Branch AFWL Kirtland AFB, New Mexico 87117	1
8. J.C.P. McEachen Naval Sea System Command Code SEA06T Washington, D.C. 20360	1
9. Lt. R.B. Birchfield Naval Material Command Code MAT 034 Washington, D.C. 20360	1

10. Dr. R.C. Hansen 1
17100 Ventura Boulevard, Sute 218
Encino, California 91316
11. Dr. Don Dudley 1
Department of Electrical Engineering
University of Arizona
Tuscon, Arizona 87521
12. Dr. A. Sankar 1
MS R-1 1144
TRW System, 1 Space Park
Redondo Beach, California 90278
13. Al Mink Code 6174 1
Fran Prout, Code 6174 1
Tony Testa, Code 6174 1
Dr. S. Siahatgar, Code 6174 1
Naval Ships Engineering Center
Hyatts, Maryland 20784
14. Ronald Prehoda, Code FVR 1
Naval Surface Weapons Center
Dahlgren, Virginia 22448
15. Cdr. E.G. Neely III 1
Naval Electronic System Command
Code ELEX 094
Washington, D.C. 20360
16. Dr. R. Tanner 1
Technology for Communication International
1625 Stierlin Road
Mt. View, California 94043
17. Dr. Fred Tesche 1
Science Application, Inc.
P.O. Box 277
Berkeley, California 94701
18. Walter Curtis 1
Boeing Aerospace Company
P.O. Box 3999
Seattle, Washington 98124
19. Dr. Raj Mittra 1
Department of Electrical Engineering
University of Illinois
Urbana, Illinois 61801

20. Cdr. Russ Shields 1
Naval Electronic System Command
Code PME-107
Washington, D.C. 29360
21. Don Campbell 1
COMM/ADP LAB NL-H
USAECOM
Fort Monmouth, New Jersey 07793
22. Dr. B. Strait 1
Department of Electrical Engineering
111 Link Hall
Syracuse University
Syracuse, New York 13210
23. Dr. Art Sindoris 1
USAECOM
Fort Monmouth, New Jersey 07703
24. Phillip Blacksmith, Code LZR 1
AF Research Laboratory, LG Hanscom FD
Bedford, Massachusetts 01730
25. Cdr. USACEEIA 1
Attention: ACCC-CED-RP
(Edwin F. Bramel)
Fort Huachuca, Arizona 85613
26. Russell M. Brown 1
Code 5252
Naval Research Laboratory
Washington, D.C. 20390
27. Dennis E. Fessenden 1
Code SA32
US Naval Underwater System Center
New London, Connecticut 06320
28. Joseph Halberstein 1
Code FVN
Naval Weapon Laboratory
Dahlgren, Virginia 22448
29. Dr. Rudy Kalafus 1
Transportation System Center
Cambridge, Massachusetts 92143

30. Cyril M. Kaloi 1
US Naval Missile Center
Point Mugu, California 93041
31. Maj. Anthony Martinez 1
LZR
A F C R L
Hanscom Field, Massachusetts 91730
32. Dr. E.K. Miller (L158) 1
Lawrence Livermore Laboratory
P.O. Box 808
Livermore, California 94550
33. John Potenza 1
(OCTS)
Rome Air Development Center
Griffiss AFB, New York 13441
34. Dr. John W. Rockway 1
Naval Electronic Laboratory Center
Code 2120
San Diego, California 92152
35. Carlyle J. Sletten 1
Code LZ
AF Cambridge Research Laboratory
Bedford, Massachusetts 91730
36. Asst. Professor J.B. Knorr, Code 52KO 1
Department of Electrical Engineering
Naval Postgraduate School
Monterey, California 93940

Thesis

K3963

c.1

Khemayodhin

157245

Calculation of surface current on perfectly conducting bodies of arbitrary shape.

4 AUG 87

31029

Thesis

K3963

c.1

Khemayodhin

157245

Calculation of surface current on perfectly conducting bodies of arbitrary shape.

thesK3963

Calculation of surface current on perfec



3 2768 002 12151 9

DUDLEY KNOX LIBRARY